

University of Montana

## ScholarWorks at University of Montana

---

Graduate Student Theses, Dissertations, &  
Professional Papers

Graduate School


---

2021

# INVESTIGATIONS ON NOVEL CYP26A1/B1 INHIBITOR, DX308: USING atRA RESPONSE AS A THERAPUTIC TARGET FOR TRAUMATIC BRAIN INJURY AND PARKINSON'S DISEASE

Jacob Morgan Leatherwood  
*The University Of Montana*

Follow this and additional works at: <https://scholarworks.umt.edu/etd>

 Part of the [Medicinal and Pharmaceutical Chemistry Commons](#), [Nervous System Diseases Commons](#),  
and the [Pharmaceutics and Drug Design Commons](#)

**Let us know how access to this document benefits you.**

---

### Recommended Citation

Leatherwood, Jacob Morgan, "INVESTIGATIONS ON NOVEL CYP26A1/B1 INHIBITOR, DX308: USING atRA RESPONSE AS A THERAPUTIC TARGET FOR TRAUMATIC BRAIN INJURY AND PARKINSON'S DISEASE" (2021). *Graduate Student Theses, Dissertations, & Professional Papers*. 11801.  
<https://scholarworks.umt.edu/etd/11801>

This Thesis is brought to you for free and open access by the Graduate School at ScholarWorks at University of Montana. It has been accepted for inclusion in Graduate Student Theses, Dissertations, & Professional Papers by an authorized administrator of ScholarWorks at University of Montana. For more information, please contact [scholarworks@mso.umt.edu](mailto:scholarworks@mso.umt.edu).

INVESTIGATIONS ON NOVEL CYP26A1/B1 INHIBITOR, DX308: USING  $\alpha$ RA  
RESPONSE AS A THERAPUTIC TARGET FOR TRAUMATIC BRAIN INJURY AND  
PARKINSON'S DISEASE

BY

JACOB MORGAN LEATHERWOOD

B.S. Biochemistry, Roanoke College, Salem, VA, 2016  
B.S. Neuroscience, University of Montana, Missoula, MT, 2020

Thesis

presented in partial fulfillment of requirements  
for the degree of

Masters of Neuroscience

The University of Montana  
Missoula, MT

August 2021

Approved by:

Scott Whittenburg, Dean of The Graduate School  
Graduate School

Philippe J. Diaz, Chair  
Department of Biomedical and Pharmaceutical Sciences

Kasper B. Hansen  
Department of Biomedical and Pharmaceutical Sciences

Richard J. Bridges  
Department of Biological Sciences

Mark L. Grimes  
Department of Biological Sciences

Yoonhee Jang  
Department of Psychology

## Investigations of Novel CYP26A1/B1 Inhibitor, DX308: Using atRA Response as a Therapeutic Target for Traumatic Brain Injury and Parkinson's Disease

Chairperson: Philippe J. Diaz

### Abstract

Neurodegenerative diseases (NDs) take a wide spectrum of pathologies and have a tendency to present themselves later in life. Neurodegenerative diseases affect 6 million Americans annually with ~1 million currently living with Parkinson's disease (PD). One of the greatest contributors to the pathogenesis of neurodegenerative diseases is the occurrence of a traumatic brain injury (TBI) during life.

All-*trans*-retinoic acid (atRA) is the active metabolite of Vitamin A. The retinoic acid pathway is known to be activated following TBI and is reduced in PD patients. Previous studies found a decrease in inflammation and behavioral deficits following administration of Vitamin A or atRA post TBI. Retinoic acid receptor stimulation has been found to protect dopaminergic neurons of the substantia nigra. Studies have shown that endogenous atRA within brain tissue supports neuronal protection, axonal growth, inflammatory modulation, and glial differentiation. Retinoic acid metabolism blocking agents (RAMBAs) are emerging as new therapeutic interventions with the goal of increasing endogenous atRA brain concentration, for the treatment of TBI and PD.

Our hypothesis was that instead of directly activating retinoic acid receptors, inhibition of the metabolism of atRA produced after central nervous system injury will have a neuroprotective effect and reduce the development of neurodegenerative diseases or cognitive impairments induced by TBI. This research sourced a newly synthesized RAMBA, DX308, for the purpose of confirming its action as a CYP26A1/B1 inhibitor. The aim of this project was to determine DX308 binding mode, and to characterize the effect of DX308 on atRA signaling *in vitro*. Modeling DX308-CYP26A1/B1 ligand-protein interaction was performed in order to support competitive binding of DX308. Glial- and neuroblastoma cell culture experiments were the preliminary investigation into DX308 as a functional RAMBA within the central nervous system.

DX308 was shown to have a binding mode similar with tazarotenic acid, and atRA. Treatment of SNB19 and SHSY5Y cells with atRA dose dependently modulated retinoid-responsive genes. DX308 potentiated the effects of a nanomolar concentration of atRA in SNB19 however, this effect was not confirmed in SHSY5Y. Follow up experiments involving SHSY5Y atRA/TPA dopaminergic differentiation displayed an altered dopamine receptor expression compared to SHSY5Y control cells.

## Table of Contents

1. Introduction & Background.....	1
1.1 Traumatic Brain Injury.....	2
1.1.1 Signaling Cascade.....	3
1.1.2 Neuroinflammation & Gliosis.....	4
1.1.3 Oxidative Stress.....	6
1.1.4 Current Treatments.....	6
1.2 Parkinson's Disease.....	7
1.2.1 Pathology: Lewy Body Formation & Braak Staging.....	8
1.2.2 Prominent Genes.....	9
1.2.3 Inflammation.....	10
1.2.4 Nigrostriatal Pathway: Parkinsonian Dysfunction.....	10
1.2.5 Current Treatments.....	11
1.3 All-trans Retinoic Acid & Synthetic Retinoids.....	12
1.3.1 Biosynthesis, Transport & Metabolism of Endogenous Retinoids.....	12
1.3.2 atRA Regulation & Canonical Signaling.....	14
1.3.3 Non-canonical atRA Signaling.....	16
1.3.4 Retinoic Acid in the Adult Brain.....	18
2. CYP26A1/B1 & DX308 Modeling Investigations.....	19
2.1 Cytochrome P450: CYP26A1/B1.....	19
2.2 Experimental Approach: Docking of DX308 in CYP26A1/B1 Homology Models...	20
2.3 atRA & Metabolites Comparison Results.....	22
2.4 Tazarotenic Acid, R116010, & DX308 Comparison Results.....	23
3. Novel CYP26 Inhibition of Retinoic Acid Clearance via DX308.....	28
3.1 Introduction.....	28
3.2 Methods.....	29
3.2.1 SNB19-Human Glioblastoma.....	29
3.2.1.1 SNB19-Cell Culture.....	29
3.2.2 SHSY5Y-Human Neuroblastoma.....	30
3.2.2.1 SHSY5Y Cell Culture.....	30
3.2.3 Differential Gene Expression.....	31

3.2.3.1 RNA Isolation.....	31
3.2.3.2 RT-qPCR.....	32
3.3 Results.....	33
3.3.1 atRA Response in SNB19/SHSY5Y Cells.....	33
3.3.2 atRA/TPA Differentiation of SHSY5Y Effect on Dopamine Receptor Expression.....	36
3.4 Discussion.....	37
4. Conclusion and Future Directions.....	39
4.1 Conclusion.....	39
4.2 Future Directions.....	40
5. References.....	42
6. Appendices.....	53
6.1 Supplemental Data.....	53

## List of Figures

### 1. Introduction

Figure 1.1: Traumatic Brain Injury Overview.....	2
Figure 1.2: Activated Microglia as Therapeutic Target In Neurodegenerative Diseases.....	5
Figure 1.3: Braak Staging Progression in PD.....	8
Figure 1.4: Nigrostriatal Pathway.....	11
Figure 1.5: Retinoic Acid Biosynthesis Schematic.....	12
Figure 1.6: atRA Biosynthesis and Storage Pathway.....	13
Figure 1.7: Canonical RA signaling Pathway.....	14
Figure 1.8: Crystal Structure RAR $\beta$ -RXR $\alpha$ Heterodimer.....	15
Figure 1.9: MAPK Signaling Pathway Under Retinoic Acid & Growth Factor Stimulation.....	17

### 2. CYP26A1/B1 & DX308 Modeling Investigations

Figure 2.1: Molecular Modeling of CYP26A1/B1-atRA/Metabolites.....	22
Figure 2.2: Molecular Modeling CYP26A1/B1-Tazarotenic Acid.....	23
Figure 2.3: Molecular Modeling CYP26A1/B1-R116010.....	24
Figure 2.4: Molecular Modeling CYP26A1/B1-DX308.....	25

### 3. Novel CYP26 Inhibition of Retinoic Acid Clearance via DX308

Figure 3.1: SHSY5Y Differentiation Regiment.....	31
Figure 3.2: JML_101-SNB19 atRA Treatment.....	33
Figure 3.3: JML_111-SNB19-atRA/DX308.....	34
Figure 3.4: JML_127-SHSY5Y-atRA/DX308.....	35
Figure 3.5: JML_135-SHSY5Y/SHSY5YDiff-atRA/TPA Regiment.....	36
Figure 3.6: JML_141-SHSY5Y/SHSY5YDiff/SHSY5YDiffDX308.....	37

## List of Tables

### 1. Introduction

N/A

### 2. CYP26A1/B1 & DX308 Modeling

Table 2.1: Novel RAMBA Library.....19

Table 2.2: CYP26A1/B1 Modeling Measurements.....27

### 3. Novel CYP26 Inhibition of Retinoic Acid Clearance via DX308

Table 3.1: Experimental Summary.....28

Table 3.2: Primer List.....32

## List of Third Party Copyrighted Material

<b>Figure Number</b>	<b>Publisher</b>	<b>License Number</b>
Figure 1.1	Elsevier	5120960550404
Figure 1.2	Springer Nature	5117921504519
Figure 1.3	Springer Nature	5118931386497
Figure 1.5	Elsevier	5120971023697
Figure 1.7	Elsevier	5132001432519
Figure 1.8	Elsevier	5113781026721



## List of Abbreviations

<b>AP</b>	Anterior/Posterior Patterning
<b>ARG1</b>	Arginase 1
<b>ATP</b>	Adenosine Triphosphate
<b>atRA</b>	All-trans Retinoic Acid
<b>BBB</b>	Blood Brain Barrier
<b>BCMO1</b>	6-hydroxyl-dopamine 1-methyl-4-phenyl-1,2,3,6-tetrahydropyridine
<b>BDNF</b>	Brain Derived Neurotrophic Factor
<b>Ca<sup>2+</sup></b>	Calcium
<b>CaM</b>	Calmodulin
<b>CaMKII</b>	Ca <sup>2+</sup> /calmodulin-dependent Kinase 2
<b>CNS</b>	Central Nervous System
<b>CRABP1</b>	Cellular Retinoic Acid Binding Protein 1
<b>CRBP1</b>	Cellular Retinol Binding Protein 1
<b>CYP26A1</b>	Cytochrome P450, Family 26, Subfamily A, polypeptide 1
<b>CYP26B1</b>	Cytochrome P450, Family 26, Subfamily B, polypeptide 1
<b>DA</b>	Dopamine/Dopaminergic
<b>DBD</b>	DNA binding Domain
<b>DRD1,2,3</b>	Dopamine Receptors 1,2,3
<b>DV</b>	Dorsal/Ventral Patterning
<b>GABA</b>	Gamma-aminobutyric Acid
<b>GBA</b>	Beta-glucocerebrosidase
<b>GDNF</b>	Glial Derived Neurotrophic Factor
<b>GFAP</b>	Glial Acidic Fibrillary Protein
<b>Glu</b>	Glutamate
<b>GPE</b>	Globus Pallidus Externa
<b>GPI</b>	Globus Pallidus Interna
<b>GWAS</b>	Genome Wide Association Studies
<b>IL-10</b>	Interlukin-10
<b>IL-13</b>	Interlukin-13
<b>IL-1<math>\beta</math></b>	Interlukin-1 Beta
<b>IL-4</b>	Interlukin-4
<b>IL-6</b>	Interlukin-6
<b>iNOS</b>	Induced Nitrogen Oxide Synthase
<b>LBD</b>	Ligand Binding Domain
<b>LPS</b>	Lipopolysaccharide
<b>Lrat</b>	Lecithin:retinol Acyltransferase
<b>LRRK2</b>	Leucine Rich Repeat Kinase
<b>MAPK</b>	Mitogen-activated Protein Kinase
<b>MPTP</b>	6-hydroxyl-dopamine 1-methyl-4-phenyl-1,2,3,6-tetrahydropyridine
<b>Na<sup>2+</sup></b>	Sodium
<b>NCoA1</b>	Steroid Receptor Co-activator-1
<b>NMDA</b>	N-methyl-D-aspartic acid
<b>NO</b>	Nitrogen Oxide
<b>NOX2</b>	Nicotinamide Adenine Dinucleotide Phosphate Oxidase

<b>NRIDs</b>	Nuclear Receptor Interacting Domains
<b>NT</b>	Neurotransmitter
<b>PARK2</b>	Parkin
<b>PD</b>	Parkinson's Disease
<b>PINK1</b>	PTEN-induced Putative Kinase
<b>RA</b>	Retinoic Acid
<b>RALDH2</b>	Retinaldehyde Dehydrogenase
<b>RAR<math>\alpha</math>,<math>\beta</math>,<math>\gamma</math></b>	Retinoic Acid Receptor $\alpha$ , $\beta$ , $\gamma$
<b>RAREs</b>	Retinoic Acid Response Element
<b>RBPR2</b>	Retinol Binding Receptor Protein Type 2
<b>RDH</b>	Retinol Dehydrogenase
<b>Reh</b>	Retinyl Ester Hydrolase
<b>RNS</b>	Reactive Nitrogen Species
<b>ROS</b>	Reactive Oxygen Species
<b>Rrd</b>	Retinal Reductase
<b>RXR</b>	Retinoic X Receptor
<b>RYR</b>	Ryanodine Receptor
<b>SNCA</b>	Alpha-synuclein
<b>SNpc</b>	Substantia Nigra Pars Compacta
<b>STRA6</b>	Signaling receptor and Transporter of Retinol
<b>TBI</b>	Traumatic Brain Injuries
<b>TGF-<math>\beta</math></b>	Transforming Growth Factor-Beta
<b>TNF<math>\alpha</math></b>	Tumor Necrosis Factor Alpha
<b>TPA</b>	12-O-tetradecanoyl-phorbol-13-acetate
<b>TTR</b>	Transthyretin
<b>VAD</b>	Vitamin A Deprivation Diet
<b>VGCCs</b>	Voltage Gated Calcium Channels

## 1. Introduction & Background

Neurodegenerative diseases have long been a challenging area for both research scientists and healthcare professionals alike. Characterized by the progressive degeneration of a neuronal population, or group of neurons, the pathology progresses to affect cognitive and motor functions associated with the central and peripheral nervous system. Unfortunately, the prevalence of becoming diagnosed with a neurodegenerative disease increases dramatically after the age of 65 (Prince et al., 2013). Genetic and environmental factors contribute to the neurodegenerative pathophysiology with most diseases caused by protein misfolding and subsequent aggregation. Tauopathies, amyloidosis,  $\alpha$ -synucleinopathies, and other misfolded proteins all contribute to neurodegenerative diseases such as dementia, Alzheimer's, Huntington's, and Parkinson's disease (Dugger & Dickson, 2017). Adding insult to injury, traumatic brain injuries are associated with the pathogenesis of  $\alpha$ -synuclein and amyloid-beta plaque formation, resulting in neurodegenerative diseases such as Alzheimer's and Parkinson's in later years of life. While the direct mechanisms are unknown associations between the biochemical cascade, cytotoxicity, and latent traumatic brain injury signaling sequelae all point to dysfunctional homeostatic process revolving around increased inflammatory signaling (Ladak et al., 2019).

Current treatments for neurodegenerative diseases often involve barbiturates and antipsychotics that target neurotransmitter signaling and transportation, often affecting quality of life for patients (Fox et al., 2011). Recently retinoid therapy has been proposed as retinoic acid signal transduction is induced after a traumatic brain injury and is reduced in Parkinson's disease patients later on in life. All-trans retinoic acid signaling is shown to be associated with multiple genes involved in neurodegenerative pathogenesis and the inflammatory response (Goodman & Pardee, 2003). Additionally, endogenous regulation of retinoic acid in the adult brain supports neuronal protection, axonal growth, glial differentiation, and inflammatory modulation (Mey, 2006). This research investigates the potential for a novel RAMBA, DX308, to target atRA metabolism in an effort to increase endogenous all-trans retinoic acid signaling. We hope that preliminary research for DX308's use in the central nervous system will allow for future therapeutics to treat traumatic brain injuries and subsequent neurodegenerative diseases without affecting quality of life in patients.

## 1.1 Traumatic Brain Injury

Traumatic brain injuries (TBIs) are caused by blunt force trauma to the head or skull and can be classified as an open or closed injury based on the integrity of the skull and dura matter (Morrow & Pearson, 2010). The mechanical forces trigger vascular ruptures, glial/astrocyte activation, inflammation, and apoptosis resulting in neuronal tissue loss and cognitive impairment (Ladak, et al., 2019). TBIs were projected to be the third leading cause of death in 2020, with 10 million occurring worldwide annually, and the United States accounting for 1.7 million (W.H.O., 2002). The direct mechanical damage is defined as the primary

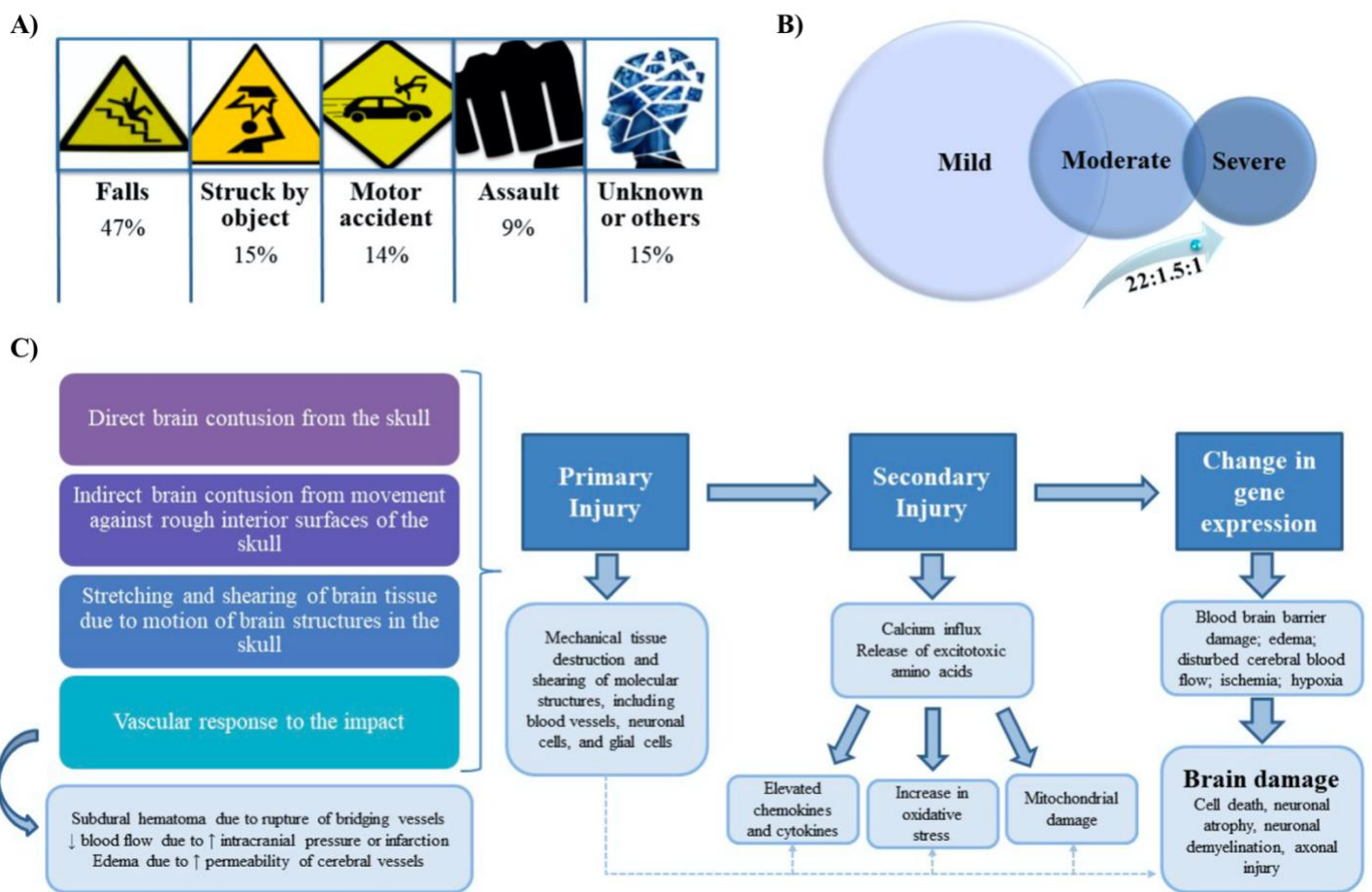


**Figure 1.1: Traumatic Brain Injury Overview.** A) Causation distribution in the United States. B) Ratio of severity. C) Primary and secondary pathophysiology and interplay.

Source: El Hayek et al. (2020), with permissions from Elsevier (lic #: 5120960550404)

(1<sup>o</sup>) insult and is characterized as the physiologic cause of cell death. This 1<sup>o</sup> injury manifests itself as damage to neuronal tissue, blood vessels, and the initiation of the biochemical cascade which leads to the secondary (2<sup>o</sup>) insult, characterized by excitotoxic cell death (Mioni et al., 2014). The 2<sup>o</sup> injury, initiated within minutes to hours after 1<sup>o</sup> insult, is characterized by the release of neurotransmitters (NT), cytokines, and transcription factors which form a biochemical signaling storm. This biochemical signaling cascade is the molecular basis for the 2<sup>o</sup> insult and causes widespread excitotoxicity in the form of nitric oxide (NO), reactive oxygen species (ROS), and inflammation that in turn initiate apoptosis and necrosis (Abdul-Muneer et al., 2015) (Figure 1.1). Traumatic brain injuries can be associated with Alzheimer's and Parkinson's disease, chronic traumatic encephalopathy, and epilepsy years to decades after the initial injury (Ladak, et al., 2019). Current treatments have a wide range of action due to the spectrum or intensity of injury. These treatments can range from raising the head and drug administration, to surgical intervention (Galgano et al., 2017). Interestingly, recent studies in the murine model show that treatment of TBI with all-trans-retinoic acid (atRA) can reduce lesion size, reactive astrogliosis, and axonal injury over seven days post injury (Hummel., et al 2020). Taken together, TBIs take on a wide spectrum of classifications and depending on the intensity of mechanical impact can produce a biochemical cascade which induces glial activation and astrogliosis resulting in cell death. Targeting the initiation and proliferation of the 2<sup>o</sup> insult is a primary target for drug intervention.

### 1.1.1 Signaling Cascade

Following the 1<sup>o</sup> insult behind a TBI the blood brain barrier and neuronal cells are compromised, and excitotoxicity takes place as glutamate (Glu) levels are elevated in the extracellular space. Working in coordination with N-methyl-D-aspartic acid (NMDA) receptors, Glu and glycine bind to the receptors to cause Ca<sup>2+</sup>/Na<sup>+</sup> influx and further downstream signaling that leads to cytotoxicity (Gao, 2016). Depolarization of neuronal populations also occurs after TBIs and can be a result of the glutamate storm from damaged vascular tissue (Hinzman et al., 2016). Membrane depolarization, caused by Ca<sup>2+</sup>/Na<sup>+</sup> influx can activate voltage gated calcium channels (VGCCs) that can increase intracellular Ca<sup>2+</sup> concentrations and strengthen depolarization (Wolf et al., 2001). Continued depolarization leads to further neurotransmitter (NT) release and a cyclical process of cytotoxic signaling occurs triggering neuronal damage or death and subsequent inflammatory response. Increased calcium levels result in activated

calpains, a cysteine protease, which is associated with cytoskeleton proteins, membrane proteins, cell adhesion molecules, and other protein kinases (Takahashi et al., 1990). Together, calpain in the presence of high  $\text{Ca}^{2+}$  concentrations compromises membrane integrity across the cell and influences signaling kinases for further downstream signaling. Sustained increased  $\text{Ca}^{2+}$  concentration further degrades the mitochondrion membrane by acting on mitochondrial permeability transition pore. Once active, this non-specific pore allows protons and  $\text{Ca}^{2+}$  to flow freely out of the mitochondria, effectively uncoupling oxidative transport chain and reducing adenosine triphosphate (ATP) synthesis. The reduction of ATP energy stores in the cell lead to further downstream signaling and necrosis (Halestrap, 2009). Once the mitochondrial membrane is compromised and ATP stores are depleted increased ROS and caspase-mediated apoptosis lead to cell death (Cheng et al., 2012). This signaling cascade begins minutes to hours after the 1<sup>o</sup> insult and is the primary therapeutic target for pharmacological intervention.

### 1.1.2 Neuroinflammation & Gliosis

Neuroinflammation is considered to be an essential part of the 2<sup>o</sup> insult response. This process involves a response mediated by microglia, and astrocytes. The release of cytokines and damage to blood vessels due to 1<sup>o</sup> mechanical insult also allows for leukocytes to invade the central nervous system (CNS). This initial response is guided by a cytokine storm that can be detrimental to neuronal survival (Hernandez et al., 2013). Resting microglia become activated in minutes after the 1<sup>o</sup> insult. Active microglia cells take the form of non-phagocytic and phagocytic phenotypic states around the area of injury. Activated microglia become polarized into M1 and M2 “classifications” respectively. M1-non-phagocytotic microglia secrete proinflammatory cytokines and neurotoxins such as:  $\text{TNF-}\alpha$ ,  $\text{IL-1}\beta$ ,  $\text{IL-6}$ ,  $\text{NO}$ , and  $\text{ROS}$ . These cytokines further damage the blood brain barrier (BBB) and signal additional inflammation downstream. M1 microglia also activate induced nitric oxide synthase (iNOS) and  $\text{Nf-kB}$  pathways which lead to neurodegeneration. In contrast, M2-phagocytotic microglia are considered to be the anti-inflammatory counterpart to M1 proinflammatory signaling. M2 microglia macrophages act to clean cellular debris and secrete anti-inflammatory cytokines:  $\text{IL-4}$ ,  $\text{IL-10}$ ,  $\text{IL-13}$ , and transforming growth factor  $\beta$  ( $\text{TGF-}\beta$ ) (Tang, 2016). These anti-inflammatory cytokines can work to combat the initial M1 inflammatory signaling. Additionally, M2 microglia are identified by Arginase 1 (Arg1) which competes with iNOS to utilize arginine for downstream signaling. iNOS uses L-arginine to produce  $\text{NO}$  and citrulline. Arg1 metabolizes L-

arginine into urea and ornithine which are precursors to hydroxyproline, proline, and polyamine. Hydroxyproline and proline are constituents of collagen synthesis and contribute to extracellular matrix and tissue repair; while some polyamines are required for cell proliferation and differentiation (Jenkins et al., 2003; Thomas & Thomas, 2001). This M1/M2 signaling competition during neuroinflammation is a prime target for TBI intervention. (Figure 1.2)

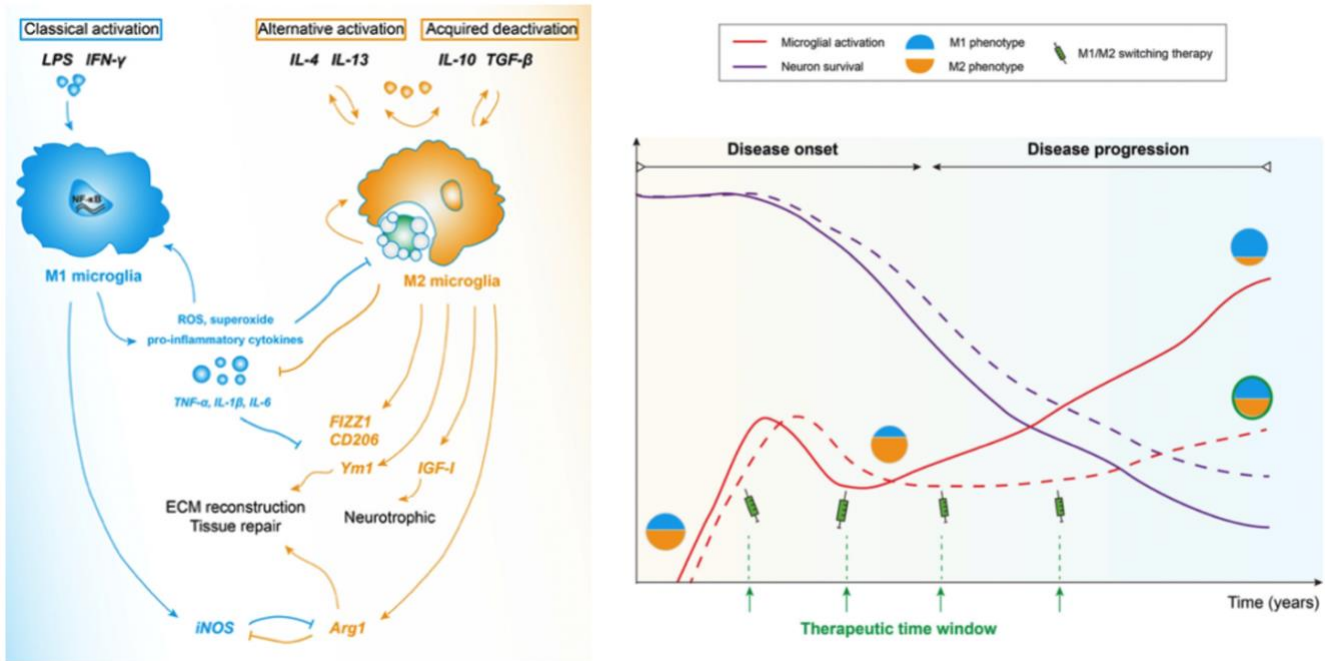


**Figure 1.2: Activated Microglia as Therapeutic Target In Neurodegenerative Diseases.** Special interest on guiding differentiation toward activated-M2-phagocytotic microglia post injury.  
 Source: Tang et al. (2016), with permission from Springer Nature (lic. #: 5117921504519)

Reactive astrocytes also play a role in the neuroinflammatory response. Astrocytes are primarily responsible for maintaining the blood brain barrier (BBB) but can also produce neurotrophic factors, regulate NT and ion concentrations, and protect against neurotoxins. Astrocytes are identified by their expression of glial fibrillary acidic protein (GFAP) and dramatically increase the expression during a TBI. Astrocytes are pivotal in the formation of a glial scar, which occurs during a severe TBI. The glial scar acts to protect the rest of the brain from the 1<sup>o</sup> insult and ensuing 2<sup>o</sup> inflammatory signaling cascade. Astrocytes also play an important role in NT reuptake, specifically glutamate and gamma-aminobutyric acid (GABA). Additionally, astrogliosis activates several signaling pathways including: JAK-STAT, Nf-kB, PI-3K/AKT, MAPK, and many more. All of which play an intersecting role in neuroinflammation of the CNS (Sonfroniew, 2009). Modification of these pathways in addition to targeting Glu and

GABA transporters is a primary focus of therapy surrounding astrogliosis (Kumar & Loane, 2012).

### 1.1.3 Oxidative Stress

Oxidative stress is a major contributor to the biochemical cascade which leads to apoptosis and necrosis following the 1<sup>o</sup> insult. Superoxide ( $O_2^-$ ) is the most common ROS following TBI and can form  $H_2O_2$  and  $OH^\cdot$ , and other ROS. After the 1<sup>o</sup> insult M1 microglia invade the damaged tissue and upregulate nicotinamide adenine dinucleotide phosphate oxidase (NOX2), subsequently producing large amounts of ROS (Kumar et al., 2016). ROS can cause a wide range of cell signaling dysfunction mediated by: DNA oxidation, lipid peroxidation, protein carbonylation, and disruption of the mitochondrial electron transport chain. Disruption of the mitochondrial membrane and electron transport chain increases ROS production and reduces available energy supplies (Cornelius et al., 2013). Lipid peroxidation damages the mitochondrial membrane and produces 4-hydroxynonenal, a byproduct that dampens astrocyte Glu receptors and  $Ca^{2+}$  ATPase activity. This effectively strengthens the 2<sup>o</sup> insult with increased extracellular Glu and intracellular  $Ca^{2+}$  concentrations aiding apoptosis and necrosis. Together, the BBB is further compromised and the 1<sup>o</sup> insult is exacerbated by increasing Glu excitotoxicity and  $Ca^{2+}$  mediated enzymatic activity (Durmaz et al., 2003; Mustafa et al., 2010).

### 1.1.4 Current Treatments

Therapeutic intervention for TBIs takes into account several aspects and characteristics of the injury. Mild TBI, or concussions, can be treated with something as simple as rest and sleep. Most TBIs are diagnosed with magnetic resonance imaging technique. Moderate to severe TBIs may require immediate surgical intervention and can use biomarkers to better understand the 2<sup>o</sup> biochemical cascade that is occurring. TBI markers can be found in the blood or cerebral spinal fluid and include: GFAP, S100B protein, caspase-3, brain derived neurotrophic factor (BDNF), neuron-specific enolase, tau, glutamate, lactate, and others (Lorente, 2017). Current drug interventions such as barbiturates or prophylactics aim to lower the metabolic demand of the brain and decrease seizure events during early TBIs respectively (Galgano et al., 2017). Further interventions try and combat the biochemical cascade that occurs after the 1<sup>o</sup> insult which can have lasting effects for years. N-type calcium channel blockers such as, ziconotide, can improve mitochondrial function; while hyperosmolar drugs like mannitol work to decrease intracranial



pressure. Amantadine is a NMDA receptor antagonist and combats Glu mediated excitotoxicity by halting the flow of ions into the neuron. Interestingly, stem cell therapy could be an option for TBI. Grafting stem and progenitor cells to the damaged areas of CNS result in improved neuronal recovery (Galgano et al., 2017). Other novel drugs like anti-inflammatory molecule MW-151 are being tested in the murine model to alter cytokine signaling and microglia/astrocyte activation (Bachstetter et al., 2012). Novel drugs include NOX2 inhibitors which seem to favor M2 differentiation and proliferation in the mouse model by combating the production of ROS via M1 microglia activation (Kumar et al., 2016). Retinoid therapy has also been proposed for TBI intervention, with particular interest on attenuating the 2<sup>o</sup> insult. Retinoic acid (RA) signal transduction has been shown to be activated when contusions, compressions, and lacerations occur in the nervous system (Mey, 2006). Recent studies show that endogenous RA in the brain supports neuronal protection, reduces axonal injury, and attenuates inflammatory signaling (Hummel et al., 2020). Targeting atRA metabolism by administering a small molecule CYP26A1/B1 inhibitor can endogenously increase atRA concentration, and possibly induce neuroprotective pathways.

## 1.2 Parkinson's Disease

Parkinson's disease (PD) was first discovered by James Parkinson in 1817 and was later diagnosed by the hallmark "shaking palsy" (Obeso et al., 2017). PD is known to be caused by the death of dopaminergic neurons in the substantia nigra pars compacta (SNpc) within the basal ganglia. Genetic factors are thought to underlie familial PD while sporadic PD is less understood and may have environmental underpinnings. Dopaminergic neurons of the SNpc project onto the striatum and release dopamine in order to regulate smooth motor movement. Because of cell death in the SNpc dopamine signaling is disrupted and PD patients present with motor dysfunction such as: tremors, rigidity, bradykinesia, swallowing, and speech difficulties (Armstrong & Okun, 2020). Other non-motor dysfunctions such as insomnia, depression, REM sleep disorder, and constipation can predate the onset of motor issues as far back as ten years (Goldman & Guerra, 2020). Age is a prevalent factor with frequency increasing almost exponentially over time, peaking at 80 years old (Driver et al., 2009). Environmental factors such as pesticide exposure, TBI, rural living and agricultural occupation,  $\beta$ -blocker use, and well-water drinking all increase the risk of PD. Interestingly; tobacco smoking, coffee drinking, non-steroidal anti-inflammatory drug use, calcium channel blocker use, and alcohol consumption all

reduce the risk of PD (Noyce et al., 2012). Genetics play a major role in contributing to the prevalence of PD. The first gene discovered to be associated with familial inherited PD encodes  $\alpha$ -synuclein (SNCA) (Polymeropoulos, 1997). Leucine rich repeat kinase 2 (LRRK2) is the most common cause of dominantly inherited PD while parkin (PARK2) is the most common cause behind recessive familial inheritance. (Corti et al., 2011)  $\beta$ -glucocerebrosidase (GBA) was found to be the highest genetic risk factor associated with the development of PD (Sidransky & Lopez, 2012). Taken together, genome wide association studies (GWAS) found single-nucleotide polymorphisms within 24 loci, including the genes mentioned above, to be associated with developing PD (IPDGC et al, 2014). More than 10 million people are living with PD globally, and nearly 1 million Americans are living with PD while 60,000 cases occur annually in the USA (Marras et al., 2018).

### 1.2.1 Pathology: Lewy Body Formation/Braak Staging

Lewy body formation within the SNpc has been the historical hallmark of PD diagnosis. Lewy bodies consist of the abnormal formation of  $\alpha$ -synuclein (SNCA) aggregates, either in the cell body (Lewy bodies) or

neurite (Lewy neurites). Missense mutations of the SNCA gene are associated with autosomal PD. Missense mutations can cause a substitution of an amino acid resulting in altered protein functions. Additionally, multiplications of the gene locus can result in over transcription. In either case the result is SNCA aggregation and the eventual formation of Lewy bodies (Devine et al., 2011). Over time, Lewy body formation follows Braak staging hypothesis. In a caudal-rostral direction starting in the peripheral nervous system and olfactory nuclei (Stage 1), Lewy

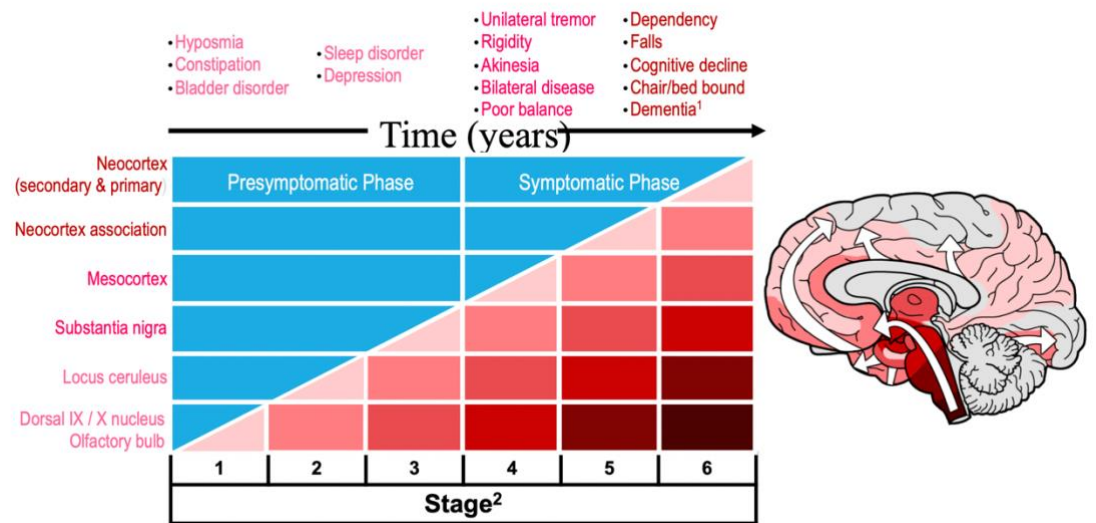


**Figure 1.3: Braak Staging Progression in PD.**  $\alpha$ -synuclein (SNCA) aggregates into Lewy bodies/neurites beginning in the peripheral nervous system (Stage 1), ending in complete innervation of the cerebral cortex (Stage 6).  
Source: Braak et al. (2002), with permission from Spring Nature (lic #: 5118931386497)

bodies begin to aggregate and progressively affect the CNS. Next, innervating the pons and spinal cord gray matter (Stage 2), and affecting the midbrain, limbic system, and basal forebrain (Stage 3). After the limbic system, Lewy bodies can be found within the thalamus and temporal cortex (Stage 4), with other aggregates forming across the cortical regions in the final stage (Stage 5) (Braak et al., 2003) (Figure 1.3). SNCA aggregation and resulting Lewy body formation is thought to cause cell death by mitochondrial and nuclear degradation (Power et al., 2017). Additionally, Lewy neurites have been attributed to synaptic dysfunction and NT deprivation (Schulz-Schaeffer, 2010). Interestingly, SNCA is expressed in the enteric nervous system with levels increasing with age. Elevated levels of misfolded SNCA is also observed in the intestines of PD patients (Bottner et al., 2012). This may be a factor of the preliminary non-motor dysfunction surrounding constipation and supports the emerging importance of the gut brain axis for PD pathology.

### 1.2.2 Prominent Genes

While SNCA mutation in PD is considered rare, the identification of Lewy bodies led to the discovery of other genes associated with monogenic PD (Corti et al., 2011). The most common gene associated with autosomal dominant inherited PD, LRRK2, predominately undergoes missense mutation, Gly2019Ser, which causes an increase in kinase activity (Ozelius et al., 2006). LRRK2 belongs to the leucine-rich repeat kinase family and is involved in multiple cellular processes ranging from neurite outgrowth and membrane trafficking to autophagy and protein synthesis (Cookson, 2012; Sanna et al., 2012). Gly2019Ser mutations of LRRK2 gene in *Drosophila* reveal pathogenic effects resulting in targeted dopaminergic neuronal cell loss and motor locomotion dysfunction (Liu et al., 2008). Other genes that are associated with autosomal recessive PD have been identified as well. Autosomal recessive inherited Parkinsonism is associated with early onset PD, before 40 years old (Schrag & Schott, 2006). PARK2 is an E3 ubiquitin ligase that works in coordination with PTEN-induced putative kinase 1 (PINK1) to break down and dispose of damaged or polarized mitochondria. Mutations to these proteins causes mitochondrial damage and impaired clearance, oxidative stress, and inappropriate  $Ca^{2+}$  signaling. All of these factors contribute to neuronal dysfunction and the cell death leading to PD pathology (McCoy & Cookson, 2012). Taken together, the genetic constituents that underlay the pathogenesis of PD revolve around protein aggregation, membrane trafficking, mitophagy/autophagy systems, and mitochondrial health. Observing genetic and molecular

mechanisms involving PD pathogenesis also lead to the use of 6-hydroxyl-dopamine 1-methyl-4-phenyl-1,2,3,6-tetrahydropyridine (MPTP) as a model for mitochondrial dysfunction (Smeyne & Lewis, 2005).

### 1.2.3 Inflammation

PD is marked by cell death in the SNpc with additional dopamine (DA) signaling dysfunction to the striatum. Genetic mutations and environmental factors cause neurodegeneration and Lewy body formation with neuroinflammation playing a central role in PD pathology. Innate and adaptive immune systems are active in the CNS inflammatory response. Although the brain has a “privileged” immune system, CD4<sup>+</sup> and CD8<sup>+</sup> T-lymphocytes are observed in the SNpc of PD patients in addition to MPTP treated mice (Brochard et al., 2008). Neurodegeneration activates microglia, gliosis, which allows for active signaling of neurotrophic factors and cytokines. Important neurotrophic factors such as: BDNF, and glial-derived neurotrophic factor (GDNF) are released from activated microglia (Batchelor, 2002). BDNF and GDNF are well known to be essential for DA neuronal survival. In vivo and in vitro models of PD support the neuroprotective effect of these neurotrophic factors on DA neurons of the SNpc, mediated by activated microglia (Kirschner et al., 1996; Tomac et al., 1995). In stark contrast to the beneficial effects of activated microglia, gliosis often results in the release of neurotoxins such as: reactive oxygen/nitrogen species (ROS/RNS), tumor necrosis factor-alpha (TNF- $\alpha$ ), and interleukin-1-beta (IL-1 $\beta$ ) (Long-Smith et al., 2009). Incorporating neuroinflammation into PD pathology is an important aspect when considering treatment and therapeutic targets. Targeting the SNpc with neurotrophic signaling constituents could save DA neurons and the downstream effect on motor control in the nigrostriatal pathway.

### 1.2.4 Nigrostriatal Pathway: Parkinsonian Dysfunction

The complete understanding of genetic and environmental factors associated with PD are still lacking in many areas; however, the pathogenesis of PD does rely on the death of dopaminergic neurons in the SNpc and subsequent loss of dopaminergic signaling to the striatum. The nigrostriatal pathway is dependent on the homeostasis of the dopaminergic neurons within the SNpc and dysregulation of DA signaling can result in loss of motor control. Within the basal ganglia the SNpc projects dopaminergic neurons towards the caudate nucleus and caudate putamen, together called the striatum. While input to the striatum originates from the SNpc and cortex, output from the basal ganglia is directed toward the thalamus via GABAergic

neurons from the globus pallidus interna (GPI). The thalamus directs nigrostriatal signaling towards the cortex for smooth movement muscle coordination. The cortex projects glutaminergic neurons to the striatum, while the striatum projects GABAergic neurons to the GPI and globus pallidus externa (GPE). The GPE then projects GABAergic neurons onto the subthalamic nucleus, which in turn projects glutaminergic neurons back onto the GPE and GPI. It is important to note that the striatal GABAergic neurons which project to the GPI express dopamine-1 receptors (DRD1) while striatal neuronal projections to the GPE express dopamine-2 receptors (DRD2). These striatal projections are considered the direct and indirect sequence for the nigrostriatal pathway, respectively (Figure 1.4). DRD1 are excitatory receptors while DRD2 receptors are considered inhibitory. When normal DA is present within the striatum, the direct pathway takes control of inhibitory projection to the GPI, causing active signaling through the thalamo-cortical spinal pathway. PD pathogenesis arises when DA neurons of SNpc die due to genetic and environmental reasons

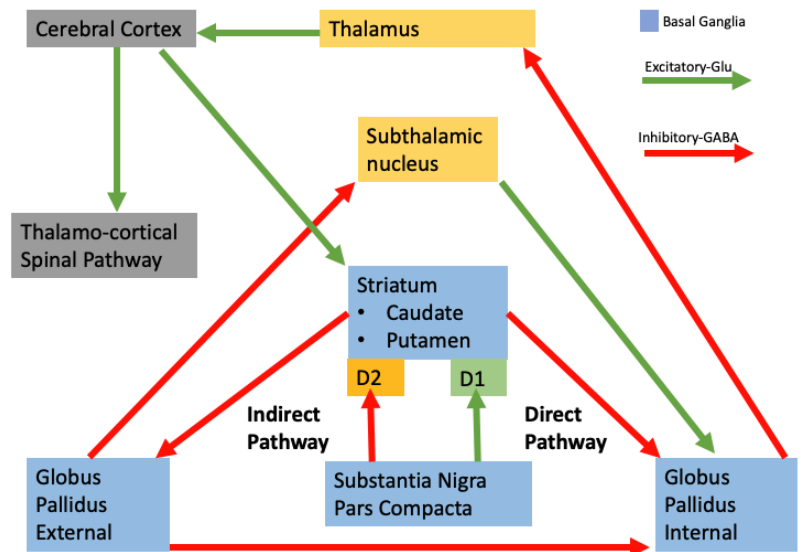


**Figure 1.4: Nigrostriatal Pathway.** The direct pathway is favored during normal dopamine release from substantia nigra pars compacta to facilitate smooth muscle movement. The indirect pathway is favored during PD pathogenesis due to lack of dopamine signaling.

discussed above. Once DA signaling is reduced or absent the excitatory/inhibitory projections from the striatum, mediated by DRD1/DRD2 receptors, becomes dysfunctional. Specifically, the indirect pathway takes precedence and causes glutaminergic projections from the subthalamic nucleus to become active, thus exciting GABAergic projections from GPI onto the Thalamus. This dysfunctional excitation of the GPI causes inhibition of thalamic output to the cortex, phenotypically observed as dysfunctional smooth muscle movement or “shaking palsy” (Harris et al., 2020).

### 1.2.5 Current treatments

Current interventions for PD are targeted toward treatment of symptoms with the aim of improving quality of life. These therapies often target the DA system including receptors and transporters. Levodopa, a BBB permeable dopamine precursor is used for severe symptoms of

bradykinesia. Since dopamine cannot cross the BBB levodopa is administered in coordination with carbidopa, a deoxy-carboxylase inhibitor, in order to prevent the peripheral conversion of levodopa to its active metabolite, dopamine, before crossing the BBB. Anti-cholinergic drugs such as clozapine can be used to treat tremors. Unfortunately, these drugs have adverse reactions. Dopamine agonists and anticholinergic drugs can cause nausea, daytime sleepiness, hallucinations, and compulsive behaviors. Long term treatment seeks to balance dopamine concentration fluctuations over time by using monoamine oxidase- $\beta$  inhibitors in coordination with other pharmaceuticals (Fox et al., 2011). Treatment of non-motor symptoms associated with PD often target depression. Venlafaxine is a serotonin and norepinephrine reuptake inhibitor and pramipexole, a dopamine agonist, seem to be effective in treating depression in PD patients (Richard et al., 2012; Barone et al., 2010). Interestingly, aged mice have decreased mRNA levels of genes necessary for atRA synthesis and metabolism: *Lrat*, *Reh*, *RALDH2*, *CYP26A1*. Treatment of Vitamin A also resorted memory performance and hippocampal neuronal morphology, suggesting that all-trans retinoic acid (atRA) signaling is diminished with age (Dumetz et al., 2020). Furthermore, studies using retinoic acid receptor ( $RAR\alpha/\beta$ ) agonists show protection of midbrain dopaminergic neurons following lipopolysaccharide (LPS) induced toxicity studies. Oral administration of tamibarotene (Am80), an  $RAR\alpha/\beta$  agonist, also prevented dopaminergic cell loss in the substantia nigra (Katsuki et al., 2009). Together this research points toward atRA therapy as a possible mediator of PD pathogenesis. Small molecule *CYP26A1/B1* inhibitors can raise the endogenous levels of atRA in the cell and mitigate the loss of retinoid signaling observed in ageing individuals or patients with PD. Additionally, atRA signaling could rescue dopaminergic neurons in the SNpc from apoptosis and prevent neuronal loss in PD patients.

### 1.3 All-trans Retinoic Acid

#### 1.3.1 Biosynthesis, Transport, & Metabolism of Endogenous Retinoids

All-trans retinoic acid is an active metabolite of Vitamin A (retinol). Retinol is a fat-soluble retinoid derived from a diet containing provitamin A carotenoids,

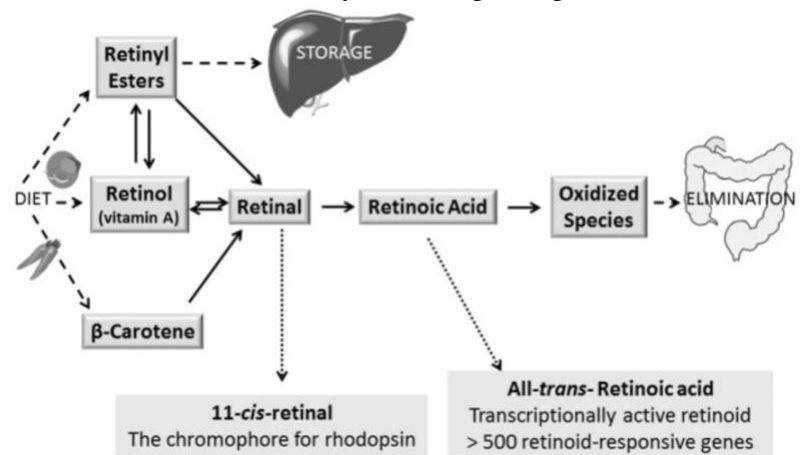


**Figure 1.5: Retinoic Acid Biosynthesis Schematic.** Vegetables and meats contain the source of carotenoids and retinyl esters respectively. Both are used for the biosynthesis of retinoic acid. Retinoids are stored as retinyl esters, predominantly in the liver. Source: Libein et al. (2017), with permission from Elsevier (lic. #: 5120971023697)

primarily  $\beta$ -carotene (D'Ambrosio et al., 2011) (Figure 1.5). Bioconversion of  $\beta$ -carotene into retinal primarily occurs in the small intestine enterocyte and is also thought to occur in the liver (Tang et al., 2003). Initially  $\beta$ -carotene undergoes symmetric oxidative cleavage at the 15,15' double bond via beta-carotene oxygenase 1 (BCMO1) to form two molecules of retinal. Further reduction by retinal reductase (Rrd) forms retinol, the predominate transport retinoid for blood circulation (Tang et al., 2003). Due to its hydrophobic nature retinol forms a trimer with retinol-binding protein 4 (RBP4) and transthyretin (TTR) in a 1:1:1 ratio in order to halt filtration in the kidneys (Raghu & Sivakumar, 2004).

Storage occurs primarily in the liver with active conversion of retinol into retinyl esters via lecithin:retinol acyl transferase (LRAT). Two transmembrane receptors, signaling receptor and transporter of retinol (STRA6) and retinol binding receptor protein (RBPR2), can uptake and convey extracellular retinol to cellular retinol binding protein type 1 (CRBP1), the intracellular retinol carrier protein. At this point intracellularly, two separate oxidation reactions occur in order to form atRA. Starting with holo-CRBP1, retinol is

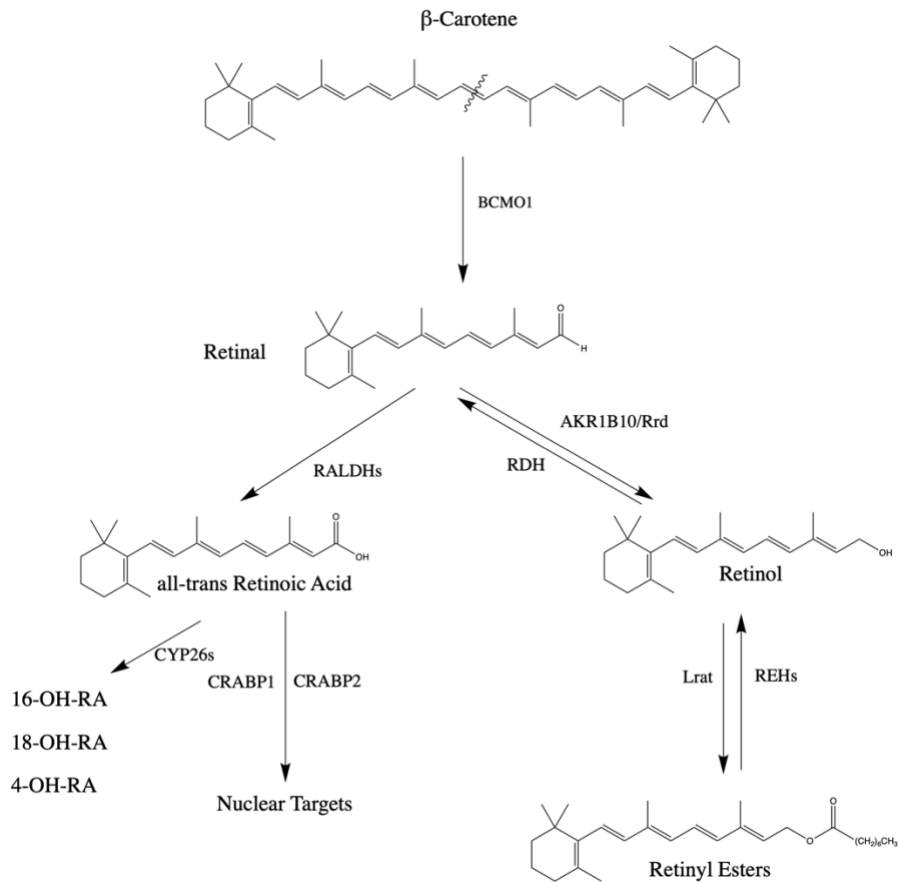


**Figure 1.6: atRA Biosynthesis, Signaling, & Storage Pathway.** Retinol enters cell and is oxidized twice to form atRA. RALDH is irreversible oxidation step in atRA synthesis.

oxidized by retinol dehydrogenase (RDH) in a protein-protein interaction to form retinal, still bound to holo-CRBP1. Depending on RDH subtype this can occur in a microsome (RDH1) or lipid droplet (RDH10) within the cell. From there the irreversible conversion of retinal into atRA is carried out by retinal dehydrogenase (RALDH<sub>1,2,3</sub>), again in a protein-protein interaction (Napoli, 2020) (Figure 1.6). Once atRA is formed the cellular retinoic acid binding protein (CRABP2) transports atRA into the nucleus for atRA directed signaling with subsequent retinoic acid receptors (RARs) located on retinoic acid

receptor elements (RAREs) (Napoli, 2017) (Figure 1.7). Degradation of atRA occurs between CRABP1 and cytochrome P450 (CYP26A1/B1) enzymes at the surface of the endoplasmic reticulum and creates hydroxyl retinoic acid metabolites (Figure 1.6).

Several factors influence this system; either driving the pathway forward toward biosynthesis of atRA, or in reverse; ending with retinyl ester storage. CRBP1-apo/holo ratio has significant control over the activation of LRAT. Where apo-CRBP1 at ~2 $\mu$ M causes LRAT inhibition, driving RDH mediated formation of retinal via protein-protein interaction with retinol-holo-CRBP1. A high concentration of apo-CRBP1 drives the atRA biosynthesis pathway forward by making retinal available for the irreversible oxidation by RALDH into atRA, while also halting the storage of retinol into retinyl esters. In contrast, atRA self regulates its intracellular concentration by inducing CYP26s (CYP26A1/B1/C1) and Lrat transcription, effectively directing the pathway toward atRA metabolism and retinyl easter storage, respectively (Napoli, 2020). Interestingly, retinol and atRA are considered teratogenic and exhibit hormesis. Hormesis is characterized by a beneficially effective dosage following an upside down “J” curve, where increasing low dosage enters a “goldilocks” zone before additional dose increases cause toxicity at high concentrations (Hayes, 2007). For healthy adults atRA plasma concentrations are around 2nM with 1 $\mu$ M being the peak concentration for therapeutic doses (Jing et al., 2016; Adamson et al., 1995). The biosynthesis, transport, and metabolism of retinoids must be highly regulated in order for proper transcription of gene targets.

### 1.3.2 atRA Regulation & Canonical Signaling

After biosynthesis of atRA is completed in the cytosol, holo-CRABP2 moves into the nucleus and directs atRA to retinoic acid receptors RAR $_{\alpha,\beta,\gamma}$  (RARs) via protein-protein interaction. In contrast, CRABP1 does not associate with RARs in the nucleus, but instead transfers atRA through diffusion (Napoli, 2017). atRA signaling takes place in the nucleus and is mediated through RAR/RXR dimer signaling.

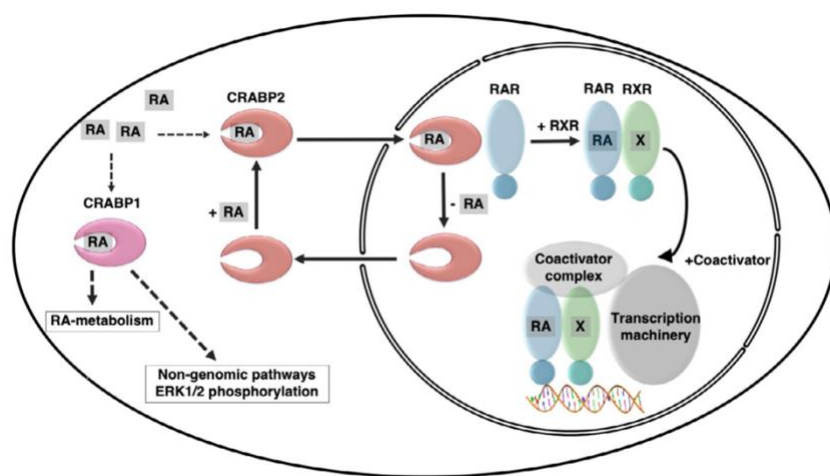


**Figure 1.7: Canonical Retinoic Acid signaling Pathway.**  
 Source: Pohl & Tomlinson (2020), with permission from Elsevier (lic #: 5132001432519)



RARs and RXRs belong to the nuclear receptor superfamily and form functional heterodimers between each other when atRA is present (Figure 1.7). Additionally, RXR/RXR homodimers can form when 9-cis-RA is present. The RAR-RXR nuclear receptors, found at retinoic acid response elements (RAREs) on the DNA, undergo conformational change when bound to atRA causing the RAR/RXR heterodimer complex to form, releasing the co-repressors, and recruiting co-activators (Germain et al., 2006a; Germain et al., 2006b). Classical RAREs are defined by a combination of hexameric motifs [(A/G)-G-(G/T)-T-C-A] designated “direct repeats 1-5” (DR1-DR5). These repeats are separated by 1, 2, or 5 base pairs (Bastien et al., 2004). Other non-canonical RAREs contain sequences with different spacing (DR0, DR8) or inverted repeats (IR0) (Moutier et al., 2012). This research utilized a GWAS study analyzing RAR $\beta$  transcriptional target sites in order to better understand downstream targets of atRA signaling in neurodegenerative diseases (Niewiadomska-Cimicka et al., 2017; Supplemental Data, Gene List 1-3).

Structurally, RAR/RXRs have a variable N-terminal domain (AF-1), a conserved DNA-binding domain (DBD), and a C-terminal ligand-binding domain (LBD). The LBD contains the ligand-dependent activation function (AF-2), which allows for coregulator interaction. Not surprisingly, the LBD also binds to atRA for dimerization to occur. The AF-1 contains phosphorylation sites that can interact with Src-homology-3 and tryptophan-tryptophan (WW) domains (Gronemeyer et al., 2004). The DBD contains two zinc binding motifs: an N-terminal recognition helix, and a DNA stabilizing helix. The LBD is organized in an “anti-

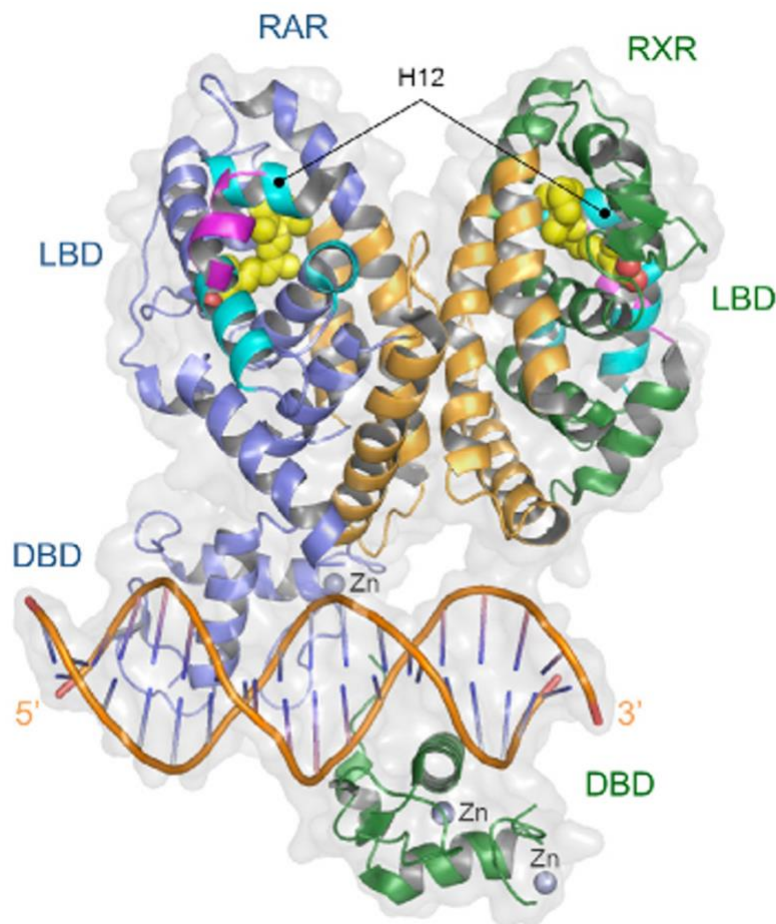


**Figure 1.8: Crystal Structure RAR $\beta$ -RXR $\alpha$  Heterodimer.** Nuclear receptors bound to DNA, ligand (RA), and coactivators. Ligands (yellow spheres), RAR-RXR co-activator binding surface (cyan, Helix 12) and dimerization surface (orange), Co-activator peptides (magenta) (PBD, 5UAN). Source: Maire et al. (2020), with permission from Elsevier (lic. #:5113781026721)

parallel  $\alpha$ -helical sandwich,” which is comprised of 12 helices (H1-H12). The H12 C-terminal helix modulates the binding of transcriptional coactivators in a ligand dependent manner (Chandra et al., 2017) (Figure 1.8).

RAR/RXR heterodimers act as transcriptional activators or repressors depending on the presence of atRA. Additionally, inverse agonists can act on RAR/RXR complex to become associated with co-repressors. Functionally, co-activators bind to RAR/RXR nuclear receptor interacting domains (NRIDs) when atRA is present in the receptor. NRIDs are comprised of three to four repeats of LxxLL motifs. Hydrophobic interactions between leucine residues and hydrogen bonds formed with RAR/RXR H3/H12 helices account for protein-protein interaction (Figure 1.8). NCoA1(steroid receptor co-activator-1) is a well-known co-activator with seven LxxL motifs (Spencer et al., 1997). Co-repressor recruitment occurs when atRA is not present and is similar to co-activator recruitment with the motif and helices changed. Importantly the H12 helix is not involved in co-repressor binding. SMRT and N-CoR (Silencing mediator of retinoic and thyroid hormone repressor, Nuclear co-repressor) are well known co-repressors that contain three functional LxxI/HIxxxI/L receptor box motifs (CoRNR 1-3). RAR/RXR H3/H4 helices form a hydrophobic surface which allows for CoRNR docking. After docking, conformational changes create an antiparallel  $\beta$ -sheet between the proteins at the N-terminus further strengthening the co-repressor interaction. (le Maire et al., 2010) In general, coactivators acetylate histones while corepressors recruit histone deacetylases (HDACs) (Heinzel et al., 1997; Nagy et al., 1997). In effect, co-activators and repressors act to relax or condense chromatin allowing for transcription or repression of regulated genes downstream. Once atRA is bound to the RAR/RXR/RARE complex co-repressors are released and co-activators are recruited followed by histone acetylation which relaxes the chromatin while RNA polymerase II is recruited for transcription of target genes. After transcription signaling is achieved RAR/RXR is ubiquitinated for degradation via a proteasome (Kopf et al., 2000). This dynamic system allows for atRA to act as signaling molecule for downstream regulation of target genes.

### 1.3.3 Non-Canonical atRA signaling

Past research has uncovered ~15,000 potential RAREs through RAR chromatin immunoprecipitation coupled sequencing (Delacroix et al., 2010; Mahony et al., 2011; Marten et al., 2010; Mendoza et al., 2011; Ross-Innes et al., 2010). Other genome-wide association studies (GWAS) identified RAR/RXR regulated genes (Al Tanoury et al., 2014; Fang et al., 2013;

Penrose et al., 2019; Niewiadomska-Cimicka et al., 2017). These sites should follow canonical gene regulation by atRA as mentioned in section above. In contrast, the non-canonical gene regulation by atRA is not mediated by RAR/RXR guided transcription but instead utilizes the CRABP1 carrier protein to modulate mitogen-activated protein kinase (MAPK) signaling (Park et al., 2019a).

In the presence of growth factors MAPK signaling pathway utilizes RAF-MEK-ERK cascade for cell growth and proliferation. In the absence of growth factor stimulation holo-CRABP1 interacts directly with rapidly accelerated fibrosarcoma kinase (RAF) to serve as a signal scaffold, conveying RAF to MEK and ERK, resulting in ERK1/2 phosphorylation. Interestingly, this also occurs under a rapid time dependent manner, peak 15 minutes, in a non-genomic fashion. Conversely, holo-CRABP1 in the presence of growth factors can act as a competitive agonist compared to RAS binding with RAF. Taken together, holo-CRABP1 can act as a modulator of MAPK

signaling in a growth factor dependent manner (Park et al., 2019a) (Figure 1.9). CRABP1 also plays a non-canonical regulatory role in cardiomyocytes when bound to atRA. In the presence of elevated intracellular calcium or isoproterenol stimulation  $Ca^{2+}$ /calmodulin (CaM) binds to CaMKII causing

autophosphorylation of T287 and autonomous kinase activity. CaMKII then goes onto phosphorylate ryanodine receptor (RyR<sub>2</sub>) on the sarcoplasmic reticulum for endogenous  $Ca^{2+}$  release. Holo-CRABP1 inhibits CaM autophosphorylation and therefore dampens the  $Ca^{2+}$  release response when atRA is present. This in turn protects against overexcitation in cardiomyocytes (Park et al., 2019b). These non-canonical atRA signaling pathways provide new therapeutic models for retinoid therapy and may be applied to the excitotoxicity following TBI.

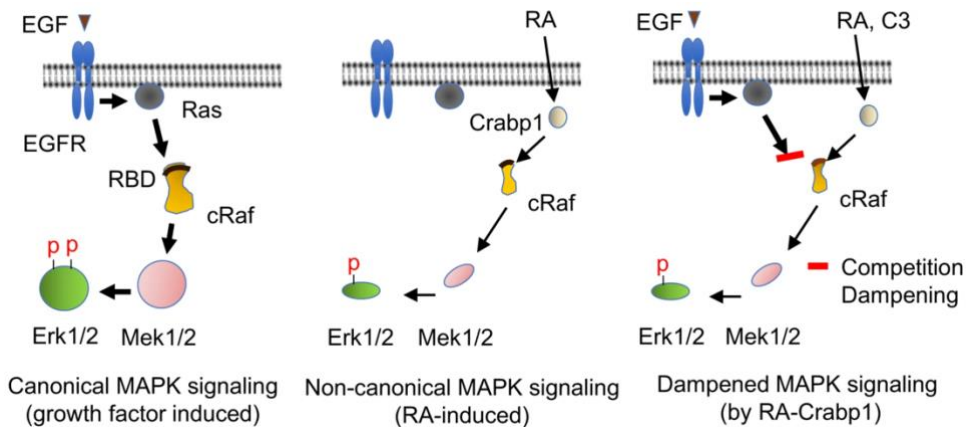


**Figure 1.9: MAPK Signaling Pathway Under Retinoic Acid & Growth Factor Stimulation.** Canonical MAPK signaling in the presence of growth factor (Left). Non-canonical MAPK signaling directed by retinoic acid when growth factor is absent (Center). RA mediated dampening of MAPK signaling as competitive agonist to Ras binding domain (Right).  
*Source: Park et al. (2019a), Springer Nature Open Access.*

### 1.3.4 Retinoic acid in the Adult Brain

Identification of RALDH expression found that stable RA synthesis in the postnatal brain mainly occurs in the basal ganglia, hippocampus and auditory afferents in the adult brain (Wagner et al., 2002). Additionally, RALDH1 is expressed throughout blood vessels in the brain while RALDH2 is found primarily in the olfactory bulb, where adult neurogenesis can occur. In coordination with possible RA synthesis in these areas, RAREs were identified in limbic structures, dorsal horn of spinal cord, and periglomerular layers of the olfactory bulb (Thompson et al., 2002). RAR receptor expression is diverse across the adult brain with RAR $\alpha$  being relatively highly expressed within the hippocampus and cortex. Interestingly, RAR $\beta$  is fairly localized to the caudate putamen and nucleus accumbens and is more highly expressed than RAR $\gamma$  (Krezel et al., 1999). RAR $\beta$  and RAR $\beta/\gamma$  knock out mice show a loss of CA1 region in the hippocampus and have reduced long-term potentiation (LTP) and long-term depression (LTD) (Chiang et al., 1998). atRA can act as a natural regulator of DRD2 receptors in developing primary striatal neurons in rats through RARE directed signaling (Valdenaire et al., 2002). This is important because DRD2 null mutation mice present with Parkinson-like motor-locomotion phenotype (Fowler et al., 2002). Additionally, RALDH1 is specifically expressed in substantia nigra neurons which synapse on the striatum (McCaffery & Drager, 1994). This is interesting because RA signaling and RALDH expression decreases with age, supporting a possible role for RA signaling in memory (Dumetz et al., 2020). Taken together the expression of atRA synthesis machinery with RARs/RAREs suggest that atRA signaling is an important factor in the regulation of neurogenesis, locomotion, memory, and learning in the adult brain. The possibility of atRA signaling rescuing dopaminergic neurons and DRD2 signaling between the substantia nigra and striatum is a primary target for PD drug interventions.

## 2. CYP26A1/B1 & DX308 Modeling Investigations

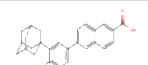
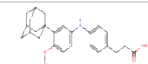
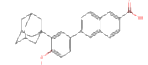
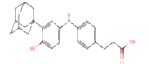
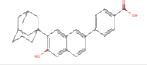
### 2.1 Cytochrome P450: CYP26A1/B1

CYP26A1 and CYP26B1 belong to the cytochrome P450 superfamily of heme-containing enzymes. Cytochrome P450 enzymes are primarily located in the membrane of the endoplasmic reticulum within liver, intestine, lung, kidney, and brain tissue (Ding & Kaminsky, 2003). Fifty-seven P450 enzymes within humans are responsible for the oxidation and reduction of most drugs used today, with the predominate isoforms identified to be: CYP1A1/A2, CYP2B6/C8/C9/C19/D6/E1, and

CYP3A4/A5 (Guengrich, 2005). Other isoforms involved in homeostatic maintenance involve: CYP4B1/F2/F12. CYP17A1, CYP19A1, CYP26A1/B1/C1. Catalytic activity requires electron donations from NADPH with additional redox constituents, cytochrome P450 reductase and cytochrome b5, to aid in the electron transfer (Schenkman & Jansson, 1999). Because of cytochrome P450 extensive mediation of drug metabolism and homeostatic functions, these enzymes are a primary target for therapeutic drug intervention. Retinoic acid metabolizing blocking agents (RAMBAs) inhibit cytochrome P450s through type II interaction which involves an sp<sup>2</sup> hybridized nitrogen for heme iron coordination (Schenkman & Jansson, 2006).

CYP26A1/B1/C1 are the predominate cytochrome P450 enzymes responsible for the oxidative metabolism of atRA. CYP26A1/B1 are expressed at low levels in most tissues of the adult human brain with the highest levels of expression observed in the pons and cerebellum (White et al., 2000). A more recent study involving the rat brain has found CYP26B1 expression within the striatum (Stoney et al., 2016). Together, the general expression of atRA metabolizing CYP26 enzymes throughout the brain with specialization occurring in the pons, cerebellum, and possibly striatum supports the homeostatic function of retinoid signaling in the brain. Targeted inhibition of CYP26A1/B1 enzymes with the specific purpose of increasing endogenous atRA concentration is the primary focus of this research. Modeling began with the comparisons of both

**Table 2.1: Novel RAMBA Library.** CYP26A1/B1 IC50 values for comparison of selective inhibitor. Special interest for structure DX308 (2) for having equal inhibition of CYP26A1 (IC50=0.05 uM) and CYP26B1 (IC50=0.05uM).

Cdid	Structure	MW	Formula	ID_Struc	CYP26A1 IC50 uM	CYP26B1 IC50 uM	A1/B1
1		398.50	C27H26O3	CD437	0.04	0.03	1.34
2		405.54	C26H31NO3	DX0308	0.05	0.05	1
3		412.53	C28H28O3	CD271	0.12	0.17	0.68
4		391.51	C25H29NO3	DX0314	1.75	0.11	16.22
5		398.50	C27H26O3	CD1530	0.53	0.8	0.65

atRA and major metabolites with a known RAMBA (R116010) and previously modeled xenobiotic substrate, tazarotenic acid. Previous research carried out in the Diaz lab positively identified CYP26A1/B1 inhibitors with repeated IC50 assays (\*data unpublished). IC50 assays were carried out by expressing CYP26A1/B1 in SF9 cells and preparing microsomal fractions. 100nM 9-*cis*-RA was used as the substrate and formation of the metabolite 9-*cis*-OH-RA was measured by HPLC. Following positive identification of CYP26 inhibitors further examination of a novel Diaz compound, DX308, was used in parallel comparison to previously known RAMBAs (Table 2.1).

## 2.2 Experimental Approach: Docking of DX308 in CYP26A1/B1 Homology Models

DX308 has been shown to inhibit CYP26A1/B1 but no experiments have been performed to show that DX308 binds to the active site of CYP26A1/B1. Our hypothesis is that DX308 bind in a similar way to natural or synthetic retinoids such as atRA and tazarotenic acid. We decided to use CYP26A1 and B1 homology models based on previous published work (Foti et al., 2016) to demonstrate that DX308 is a competitive CYP26 inhibitor mimicking retinoid structure binding modes.

Since neither CYP26A1 nor CYP26B1 has been isolated for X-ray-crystallography, homologs were used from previous research carried out by Foti et al., 2016 and Foti, Diaz & Douguet 2016. In 2016, the homology models of CYP26A1/B1 were constructed using Prime (Schrödinger LLC, New York, NY). Both amino acid sequences of human CYP26A1/B1 were sourced from NCBI protein server (Gene ID: 1592/56603). The crystalized structure of CYP120 (pdb: 2VE3) was used as a template to create both homology models. CYP26A1/B1 had 33%/34% sequence identity and 53%/54% positive sequence coverage respectively. The heme prosthetic group was ligated to Cys 442 and Cys 441 of CYP26A1 and CYP26B1 respectively. Energy minimalization was carried out with OPLS\_2005 and force-field constraints were defined within the MacroModel algorithm (Schrödinger). The homology model was structurally rationalized by evaluating Ramachandran plots and odd bond lengths and angles via PSIPRED (university College London, UK). SSPro (Schrödinger) software allowed for comparison of helical loop motifs and two-degrees-of-freedom structure characteristics to determine model flexibility. Once the homology models were created, the protein data bank (.pdb) files were used in the Foti et al., 2016a publication to identify Tazarotenic acid as a xenobiotic substrate of

CYP26A1/B1. Additionally, the .pdb files were used in the Foti, Diaz & Douguet 2016 publication to model ketoconazole and R115866. For the purposes of the current 2020-2021 research project the .pdb files were again used to compare novel CYP26A1/B1 inhibitor, DX308, against known CYP26 inhibitors; R116010, and the previous xenobiotic substrate, tazarotenic acid (Supp. Data, CYP26A1, CYP26B1 .pdb files). Both .pdb files underwent a BLAST sequence search in NCBI to confirm that we were working with 100% human CYP26A1/B1 enzymes. After confirmation, the .pdb files were used in Flare™ V3.0 modeling software for all ligand comparisons. All ligands were created in Flare™ V3.0 modeling software in addition to energy minimalization and ligand-protein docking. The docking grid was set up in an identical fashion to Foti et al., 2016a paper; where the center of the grid was placed 2-3 Å above the heme iron, with a 12 x 12 x 12 Å grid constructed around the center. Initial docking of atRA and major metabolites, 4-OH-RA and 16-OH-RA, compared active residues with previous modeling carried out by Foti et al., 2016. Further docking of Tazarotenic acid, R116010, and DX308 was performed in order to observe and compare active residues between the different modeling software. These modeling investigations intended to support DX308 as a novel RAMBA by showing similarities to the binding conformations of tazarotenic acid, R116010, and atRA metabolites with respect to the heme iron and active residues.

### 2.3 atRA substrate & Metabolite Comparison Results

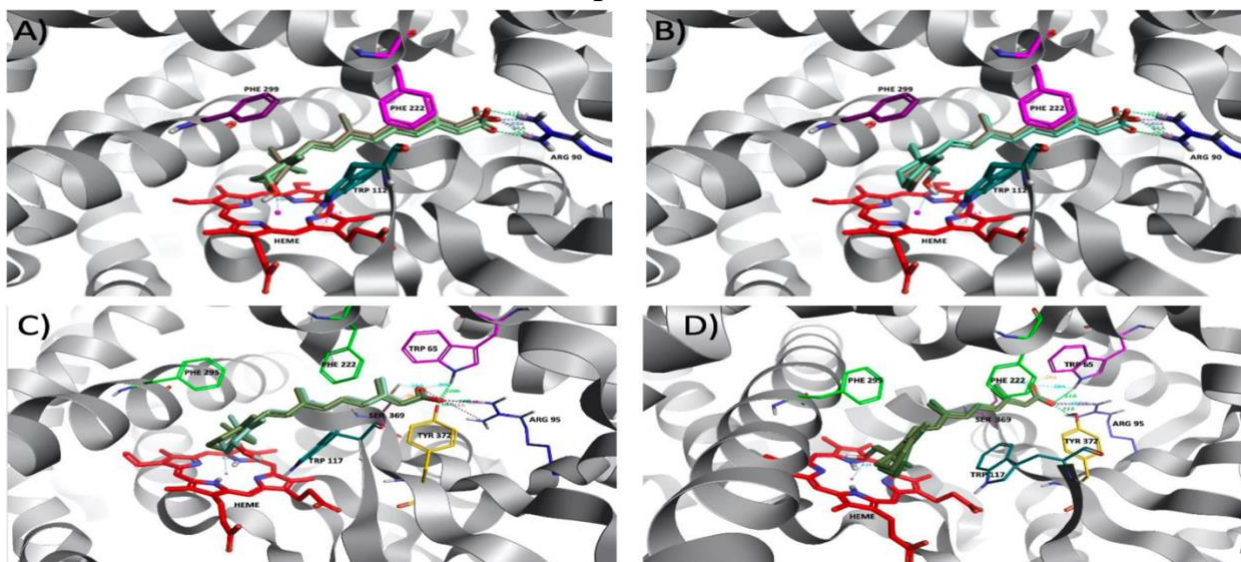


**Figure 2.1: Molecular Modeling of CYP26A1/B1-atRA/Metabolites.** CYP26A1/B1 ARG90/95 <3 Å away from carboxylic moiety. atRA metabolite favors 16-OH-RA with respect to distance from heme to active carbon (4-OH-RA: 5.6/6.5 Å vs. 16-OH-RA 3.9 Å). Distances consistent with Foti et al. (2016a). A) CYP26A1 bound atRA vs. 4-OH-RA metabolite. B) CYP26A1 bound atRA vs. 16-OH-RA metabolite. C) CYP26B1 bound atRA vs. 4-OH-RA metabolite. D) CYP26B1 bound atRA vs. 16-OH-RA metabolite.

Initial modeling investigations with the Flare™ V3.0 software overwhelmingly supported previous model docking poses observed with GlideScore and eModel (Schrödinger; Foti et al., 2016a). The primary residues involved with protein ligand interaction for atRA, 4-, and 16-OH metabolites had almost identical overlap. Trp 112, Phe 222, Phe 299, Arg 90 residues were active in the CYP26A1 binding pocket. This corresponds to Trp 117, Phe 222, Phe 295, Arg 95, Trp 65 within CYP26B1. With respect to previous modeling; Arg 90 (CYP26A1) and Arg 95, Trp 65, and Tyr 372 (CYP26B1), are all overlapping active residues that orient the carboxylic tail of atRA and the major metabolites within the 3.0 Å distance previously observed. This is also further supported by residues that orient hydrophobic the β-ionone ring toward the heme; Trp 112, Phe 222, Phe 299 (CYP26A1) and Trp117, Phe 222, Phe 295 (CYP26B1). Foti et al., 2016 also reported that 4-OH metabolite is metabolically unfavorable compared to 16-OH. This was proposed due to the measurements made between the hydrogens at 4-, 16- position of atRA relative to heme iron. Our research found similar results with 4-OH-RA to be 5.6 Å (CYP26A1) and 6.5 Å (CYP26B1) compared to 5.59 Å and 4.06 Å observed by Foti et al; while 16-OH-RA is closer to the heme iron at 3.9 Å for both CYP26A1/B1, supporting Foti et al., observations of 3.9 Å/2.9 Å for CYP26A1/B1 respectively. (Table 2.2, Figure 2.1) Taken together, these measurements support the previously observed ligand orientation relative to the active residues



within the binding pocket. Further support is warranted due to overlapping distances between specific target residues controlling carboxylic and  $\beta$ -ionone/heme ring orientation. These results are relatively significant since the docking software was different between both experiments, only sharing the original .pdb files and docking grid constraints. Further docking of previously investigated tazarotenic acid, a RAMBA, and DX308 should continue to support the viability of synthetic retinoid docking with CYP26A1/B1 enzymes.

## 2.4 Tazarotenic Acid, R116010, & DX308 Comparison Results

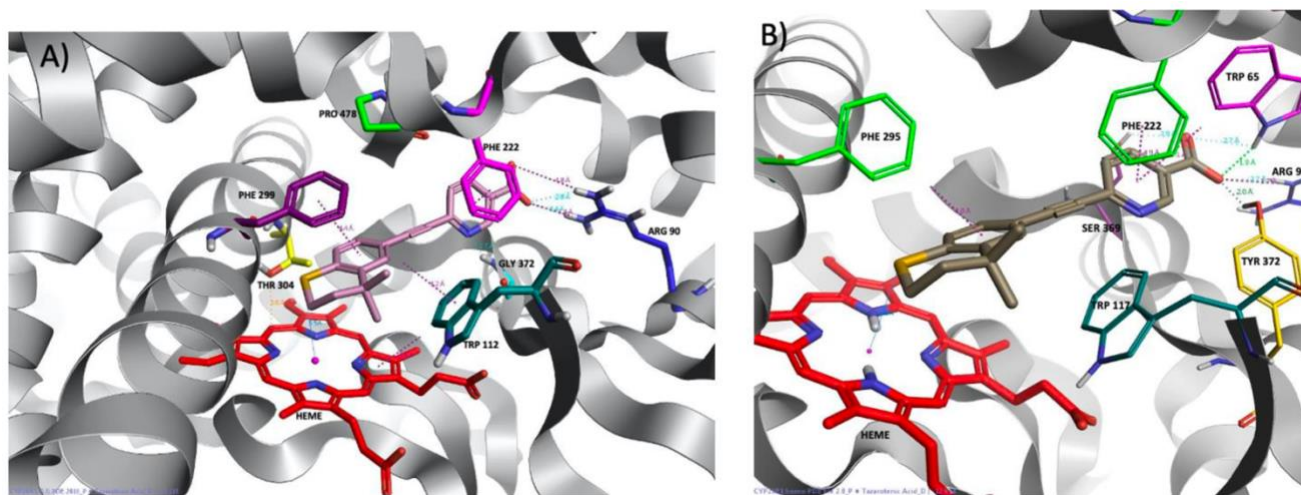


**Figure 2.2: Molecular Modeling CYP26A1/B1-Tazarotenic Acid.** Tazarotenic bound to CYP26A1/B1 in similar fashion to Foti et al (2016a) with carboxylic moiety  $<3$  Å from ARG90/95 residue and benzothiopyranyl ring oriented toward heme iron for formation of tazarotenic acid sulfoxide. A) CYP26A1 bound to tazarotenic acid. B) CYP26B1 bound to tazarotenic acid.

Modeling of Tazarotenic acid in comparison to Foti et al., 2016a further supported ligand docking orientation with respect to CYP26A1/B1 binding pocket described above. Overlap of active residues between both investigations include: Arg 90, Trp 112, Phe 222, Thr 304, Gly 372, and Pro 478 for CYP26A1; while active residues for CYP26B1 include: Arg 95, Trp 117, Phe 222, Phe 295, Tyr 372, and Trp 65. Relative distance from the sulfur atom of the benzothiopyranyl ring and the heme iron were found to be 5.5/5.9 Å compared to previously reported 4.21/4.07-4.11 Å for CYP26A1/B1 respectively. While these distances are  $>1$  Å both models report hydrogen bonding interactions between the carboxylic moiety and pyridinyl nitrogen with Arg 90 and Gly 372 of CYP26A1 respectively. (Figure 2.2, Table 2.2) Together this docking orientation overlap supports using the homology model as a rough assessment for RAMBA docking.

R116010 was used by Armstrong et al., 2007 for targeting retinoic acid metabolism in SHSY5Y neuroblastoma cell line. Our research intended to mimic the cell culturing experiment with a novel RAMBA, DX308. For this reason, R116010 compound was used in CYP26A1/B1 docking investigations to further support ligand orientation for the homology models. Specific interest was taken to observe similar active residues found to be necessary for Tazarotenic acid orientation. In coordination with active CYP26A1 residues we observed  $\pi$ -interactions between Trp 112/Phe 222 and the aromatic moieties of both ligands, R116010 and Tazarotenic acid.

Corresponding CYP26B1

residues include: Trp 117, Phe 222, and Trp 65. Additionally, work carried out by Foti, Diaz & Douget 2016b docking ketoconazole and R115866 places the  $sp^2$  hybridized nitrogen within the imidazole ring  $< 3 \text{ \AA}$  away from the heme iron. Our modeling observations of R116010 docking also shows imidazole orientation toward the heme iron at  $< 3 \text{ \AA}$ , supporting an active type II

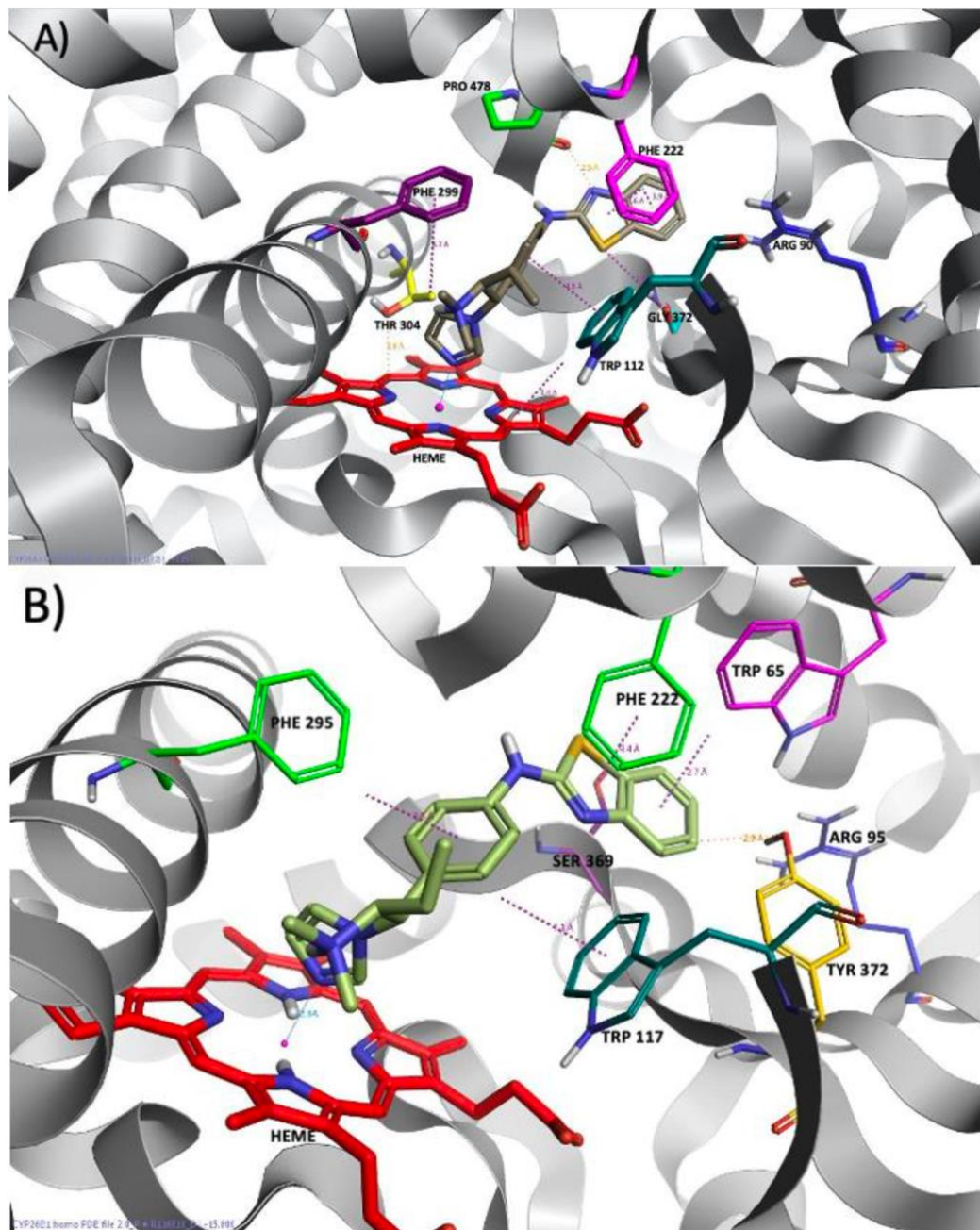


**Figure 2.3: Molecular Modeling CYP26A1/B1-R116010.** RAMBA used in SHSY5Y atRA response experiments carried out by Armstrong et al. (2007) JML\_135 modeled same cell line with different RAMBA, DX308. Ligand has loss of carboxylic orientation, gain of type II azole-heme interaction with 3-N-Heme distance  $< 3 \text{ \AA}$ . A) CYP26A1 bound to R116010. B) CYP26B1 bound to R116010.

binding interactions previously observed. (Figure 2.3, Table 2.2) Comparisons of active residue location with ligand orientation supports a heme-oriented imidazole with aromatic interactions stabilizing the rest of the molecule. Comparisons with DX308 were intended to further support this orientation and add information on the heme interactions which could possibly take place on the  $sp^2$  hybridized oxygen within the attached methoxy.

DX308, our novel CYP26A1/B1 inhibitor, had similar binding orientation with respect to all other molecules observed.

Interestingly DX308 incorporated a diverse set of residues compared to atRA, Tazarotenic acid, and R116010 alone. Active residues include: Thr 304, Trp 112, Phe 222, Pro 478, and Arg 90 for CYP26A1. Corresponding residues in CYP26B1 include: Arg 95, Trp 65, Tyr 372, and Ser 369 with Phe 295 and Trp 117 coordinating the hydrophobic adamantyl group. DX308 utilizes Arg 90/ Arg 95 hydrogen interactions with the carboxylic moiety similar to atRA, metabolites, and R116010. Additionally,  $\pi$ -interactions between aromatic moieties with Phe 222, Trp 112, Trp 117 all support bulk hydrophobic orientation toward the heme group. Finally, measurements between the heme iron and  $sp^2$  hybridized oxygen attached to benzo/adamantyl moiety is 4.0 Å/4.4 Å for CYP26A1/B1 enzymes respectively. While this is  $> 3$  Å reported by Foti, Diaz & Douget

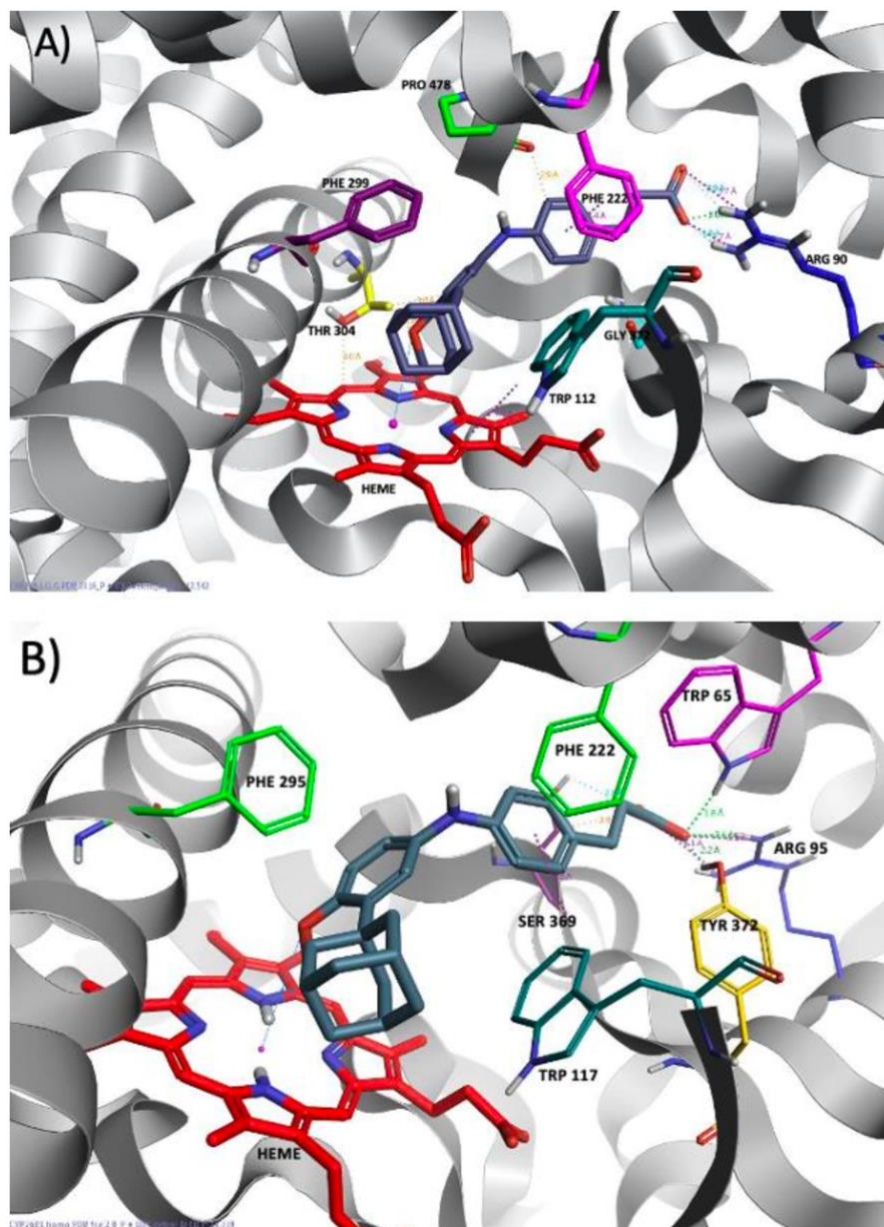


**Figure 2.4: Molecular Modeling CYP26A1/B1-DX308.** DX308 bound to CYP26A1/B1 contains multiple interactions with active residues found across previous ligands. Carboxylic moiety orients toward ARG90/95 with a distance  $< 3$  Å, hydrophobic benzo-adamantyl moiety oriented toward heme, with heme-methoxy distance 4.0/4.4 Å. A) DX308 bound to CYP26A1. B) DX308 bound to CYP26B1.

(2016) it does allow the possibility for type II binding interactions previously modeled and reported. Together DX308 is a viable candidate for inhibition of CYP26A1/B1 enzymes; furthermore, particular interest has been noted for specific analogs which allow for previously reported orientation. These include the attached adamantyl, methoxy, and butyric acid analogs needed for hydrophobic/heme orientation and carboxylic acid interactions. Generally, modeling investigations supported previous research and these homology models are an initial step in understanding the feasibility for current and future selective CYP26A1/B1 RAMBAs.

Our modeling experiments demonstrate that DX308 binds to the active site of CYP26A1 and CYP26B1 and has a similar binding mode to Tazarotenic acid and atRA forming interaction between the carboxylic acid of DX308 and residues Arg95, TYR372 and TRP65 in CYP26B1 and ARG90 in CYP26A1. These interactions are not found for R116010. Hence DX308 represents a substrate-based CYP26 inhibitor not interacting with retinoic acid receptors.

**Table 2.2: CYP26A1/B1 Modeling Measurements.** Modeling software Flare™ compared to previous work with GlideScore and eModel software (Schrödinger). Respective distances for active residues used to support DX308 active binding and inhibition of CYP26A1/B1 enzymes via type II interaction.

Substrate	CYP26A1		CYP26B1		Foti/Diaz Model	
	Residue	Distance	Residue	Distance	CYP26A1	CYP26B1
atRA	ARG 90	2-5 Å	ARG 95	2.4-4.9 Å	< 3.0 Å	< 3.0 Å
4-OH-RA	ARG 90	2-5 Å	ARG 95	2.4-4.9 Å		
	HEME-Fe	5.6 Å	HEME-Fe	6.5 Å	5.59 Å	4.06 Å
16-OH-RA	ARG 90	2-5 Å	ARG 95	2.4-3.4 Å		
	HEME-Fe	3.9 Å	HEME-Fe	3.9 Å	3.9 Å	2.99 Å
Tazarotenic Acid	PHE 299	4.4 Å	PHE 295	3.0 Å		
	PHE 222	3.5 Å	PHE 222	4.9 Å		
	ARG 90	2.4-4.8 Å	ARG 95	2.7-3.7 Å		
	TRP 112	3.2 Å	TRP 117	(4.4) Å		
	GLY 372	2.7 Å	TYR 372	2.0 Å		
	HEME-Fe	5.5 Å	TRP 65	1.9-3.7 Å		
			HEME-Fe	5.9 Å	4.21 Å	4.07-4.11 Å
R116010	PHE 299	4.8 Å	PHE 295	3.5 Å		
	PHE 222	3.6-9 Å	PHE 222	4.4 Å		
	TRP 112	4.8 Å	TRP 117	3.1 Å		
	GLY 372	3.9 Å	THR 372	2.9 Å		
	HEME-Fe	2.3 Å	TRP 65	2.7 Å		
			HEME-Fe	2.3 Å		
DX308	PHE 299	(4) Å	PHE 295	3.4 Å		
	PHE 222	3.4 Å	PHE 222	4.3 Å		
	ARG 90	1.8-3.7 Å	ARG 95	2.1-4.1 Å		
	TRP 112	(4.1) Å	TRP 117	(3.4-5) Å		
	THR 304	3.0 Å	TRP 65	1.8 Å		
	HEME-Fe	4.0 Å	SER 369	2.8 Å		
			TYR 372	2.2 Å		
			HEME-Fe	4.4 Å		

### 3. Novel CYP26 Inhibition of Retinoic Acid Clearance via DX308

**Table 3.1: Experimental Summary.** SHSY5YDiff undergoes 10uM atRA treatment day 0-3, followed by 80nM TPA treatment from day 3-6 (atRA/TPA regiment). SHSY5YDiffDX undergoes the same atRA/TPA differentiation regiment (reg.) with additional 1uM DX308 24hr treatment for a total of 7 days before harvest.

Experiment #	Type Of Cell Used	Tretments	Genes Panel
jml_101	SNB-19	0.1% DMSO: 1uM atRA: 1nM atRA	36B4, CYP26A1, CYP26B1, RARa, RARb, RARg
jml_111	SNB-19	0.1% DMSO: 1uM atRA: 1nM atRA: 100nM DX308: 1nM atRA + 100nM DX308: 10nM atRA: 10nM atRA + 10nM DX308	36B4, CYP26A1, CYP26B1, RARa, RARb, RARg
jml_127	SHSY5Y	0.1% DMSO: 100nM atRA: 10nM atRA: 1uM DX308: 100nM atRA + 1uM DX308: 10nM atRA + 1uM DX308	36B4, CYP26A1, CYP26B1, CRABP2, RARb, DRD2
jml_135	SHSY5Y+ SHSYDiff	0.1% DMSO: 10uM atRA + 80nM TPA (regiment)	36B4, CYP26A1, CYP26B1, DRD1, DRD2, DRD3
jml_141	SHSY5Y + SHSYDiff + SHSYDiffDX	0.1% DMSO: atRA/TPA: atRA/TPA + 1uM DX308	36B4, CYP26A1, CYP26B1, DRD1, DRD2, DRD3

#### 3.1 Introduction

These studies are intended to be preliminary investigations into the effects of DX308 as a novel RAMBA, primarily targeting CYP26A1/B1 atRA metabolism within the central nervous system. Previous research had selected the compound from a library of positively identified CYP26-inhibitors (Table 2.1). Further in vivo studies looked at DX308 active reduction of TBI pathology in a murine model. The purpose of this research is to test DX308 potentiation of an atRA response in order to mimic current retinoid-based therapies. This study defines an atRA response as a significant increase in gene transcription of CYP26A1 as a factor of endogenous atRA signaling (Zolfaghari, et al., 2020). RAR $_{\alpha,\beta,\gamma}$  are also used as a positive identification for active RARE signaling of prospective genetic targets (Pohl et al., 2020). Our hypothesis is that DX308 will competitively inhibit the degradation of atRA at endogenous concentration by CYP26A1/B1 in neuronal and glial cell line models. The Aim were 1) to assess the expression of CYP26A1 and CYP26B1 in SNB19 and SHSY5Y cells; 2) to characterize the effect of retinoic acid signaling activation on these two CYP26s; 3) to demonstrate that cotreatment of these cell lines with DX308 and a nanomolar concentration of RA similar to endogenous concentration will result in an increase of atRA signaling activation using CYP26A1 as a marker of direct RAR activation and CYP26B1 indirect activation; 4) to assess the effect of DX308 on the differentiation of SHSY5Y cells,

Effective potentiation of atRA via DX308 is defined within the context of an active RAMBA. In order for a RAMBA to be considered active; co-treatments of DX308 with low doses of atRA (1nM) create the same, or increased, atRA response as a high dose atRA treatment (1uM) alone compared to control. Observations of identical atRA doses will result in increased atRA response in the presence of a RAMBA. Additionally, RAMBA treatments alone

will not have an effect on atRA response. Taken together, a RAMBA treatment alone will not activate the atRA response, but under co-treatment with atRA exhibit an increase in active atRA response, indicating effective RAMBA inhibition of atRA metabolism.

This study used two human derived cell lines; neuroblastoma (SHSY5Y), and dendritic glioblastoma (SNB19). Additionally, a differentiated dopaminergic neuroblastoma (SHSY5YDiff); defined by significant increase in dopamine receptor expression relative to control, was treated. In total “three” cell lines were treated in this experiment in order to roughly model *in vivo* neuronal and glial populations. Special investigations into differentiation of the dopaminergic neuroblastoma cell line are intended to generally model dopaminergic neurons, with respect to the Parkinson’s model (Hong-Rong et al., 2010). These cell lines were used for a preliminary investigation of DX308 as a selective CYP26A1/B1 inhibitor within the central nervous system. One overall study with five independent cell culturing experiments using two cell lines was carried out culminating in the gene expression analysis of atRA response across various DX308 and atRA treatments (Table 3.1).

## 3.2 Methods

### 3.2.1 SNB19-Human Glioblastoma

SNB19 (ATCC<sup>®</sup> CDL-2219<sup>™</sup>) is a malignant glioblastoma cell line, sourced from a 47-year-old male’s left parieto-occipital glioblastoma multiforme tumor in 1980. This cell line expresses glial fibrillary acidic protein (GFAP) which acts as positive glial marker. DNA profiling studies have shown the cell line to be a derivative of U-373 cell line (ATCC<sup>®</sup> HTB-17<sup>™</sup>) which also shares derivative chromosomes with U-373 MG.

#### 3.2.1.1 SNB19-Cell Culture

The cell line was received when split during passage 19 (P19) from the Bridges Lab, University of Montana. The initial cell culture was grown to confluence of ~60% and seven cryovials, with 1.5 million cells/vial, were stored in liquid nitrogen for future experiments. All cell culture experiments were plated at P20 or higher. All culture media (cDMEM) contained: DMEM/F-12 (1:1) +2.50mM L-Glutamine ·HEPES (HyClone<sup>™</sup>, SH30271.01), 10% heat inactivated fetal bovine serum (HyClone<sup>™</sup>, AD1811280), 1% penicillin/streptomycin (Pen/Strep Corning<sup>™</sup>, 30.00CL). Cells were taken out of cryo-storage and seeded in 75cm<sup>2</sup> (T75) culture flask at 50,000 cells/mL, 15mL total. cDMEM media was changed every 3-4 days until 60-70% confluent. After respective confluency was reached cells were trypsinized (0.025%

trypsin/0.01%EDTA, Gibco<sup>®</sup>, R-001-100), neutralized (Trypsin Neutralizer Solution 1x, Gibco<sup>®</sup>, R-002-100), and counted with Countess<sup>®</sup> II Automated Cell Counter. Cells are then plated on 12-well plate (Cellstar<sup>®</sup>, 665-180) at 200,000 cells/mL with 1mL/well. After 24-48hrs cells were ~70% confluent and received 24hr treatments for each well in biological triplicates. All treatments, including controls, last 24hrs with 0.1%DMSO acting as vehicle control throughout all experiments (Table 3.1, Figure 3.2, Figure 3.3). Preparation of atRA and other photosensitive compounds were made the day of treatments, with a 20mM working stock saved in a -40<sup>o</sup>C freezer.

### 3.2.2 SHSY5Y-Neuroblastoma

SHSY5Y (ATCC<sup>®</sup> CRL-2266<sup>TM</sup>) is a neuroblastoma cell line sourced from a four-year-old female's bone marrow. The original metastatic bone tumor biopsy comprised of SK-N-SH (ATCC<sup>®</sup> HTB-11<sup>TM</sup>) cells and was subcloned three times: initially to SH-SY, followed by SH-SY5, and finally to SH-SY5Y in 1970. Importantly SHSY5Y cell cultures contain adherent and non-adherent cells and can be differentiated under specific treatment regiments into mature neuron-like phenotypes (Kovalevich & Langford, 2013).

#### 3.2.2.1 SHSY5Y-Cell Culture

The cell line was thawed from cryo-storage in liquid nitrogen after previous studies conducted by Dr. Joachim Veit in January 2018 at passage 8 (P8). The Cryovial was thawed in cDMEM media, DMEM/F-12 (1:1) +2.50mM L-Glutamine ·HEPES (HyClone<sup>TM</sup>, SH30271.01), 10% heat inactivated fetal bovine serum (H.I. FBS) (HyClone<sup>TM</sup>, AD1811280), 1% penicillin/streptomycin (Pen/Strep Corning<sup>TM</sup>, 30.00CL), and grown to ~70% confluency in a T75 flask before freezing multiple vials for storage and future experiments. Freezing media contained: 90% H.I. FBS (HyClone<sup>TM</sup>, AD1811280), 10% DMSO (Fisher BioReagents<sup>TM</sup>, BP231-100).

After growing to ~70% confluency in T75 flask adherent and non-adherent cells are trypsinized, neutralized, and plated in 12-well plate. An initial experiment with undifferentiated SHSY5Y cells (SHSY5Y) was seeded at 200,000 cell/mL with 1mL/well. After 24-48hrs cells were ~70% confluent and received 24hr treatments for each well in biological triplicates. Treatments last 24hrs with 0.1%DMSO acting as vehicle control throughout all experiments (Table 3.1, Figure 3.4).



Following the initial investigations of SHSY5Y cell line; a differentiation protocol following Presgraves et al., 2004 was followed in order for “SHSY5YDiff cells to exhibit characteristics consistent with cultured dopaminergic neurons”.

After growing to ~70% confluency in T75 flask adherent and non-adherent cells were trypsinized, neutralized, and plated in 12-well plate at 100,000 cells/ml with 1ml/well. The control treatment group was plated in 0.1%

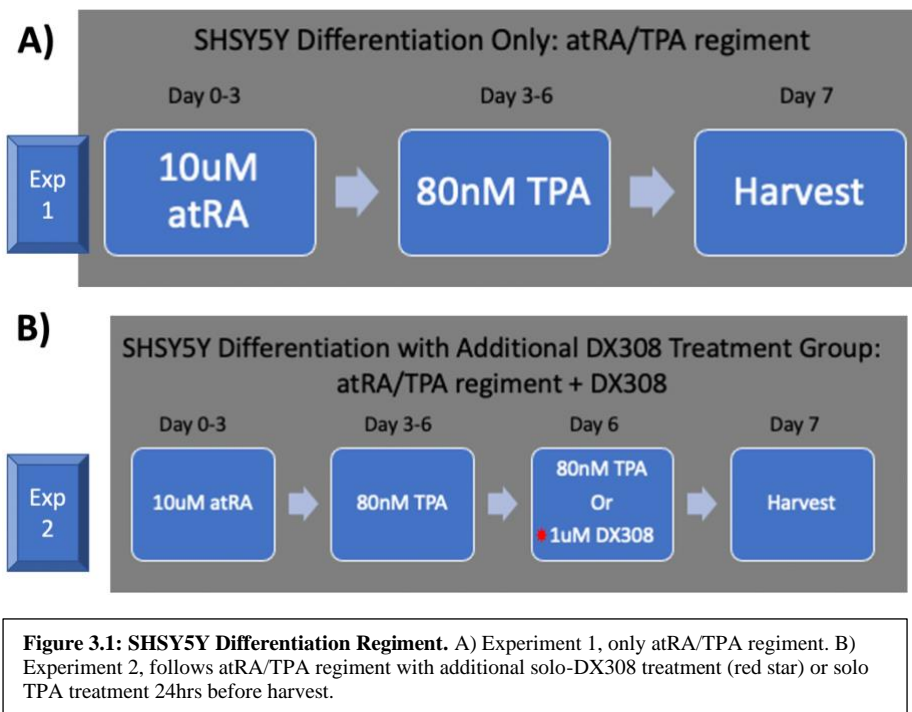
DMSO cDMEM media for 7 days, with fresh media changed on day 3. SHSY5YDiff cells were plated in 10uM atRA cDMEM media, this media was changed to 80nM 12-O-tetradecanoyl-phorbol-13-acetate (TPA) on day 3. All cells were harvested on day 7 for RNA extraction and qPCR analysis, with special interest on increased dopamine receptor (DRD<sub>1,2,3</sub>) expression with multiple comparisons (Table 3.1, Figure 3.1-Exp. 1, Figure 3.5).

The final investigation using SHSY5Y cells involved comparisons between SHSY5Y cells and SHSY5YDiff cells with respect to atRA response and DRD<sub>1,2,3</sub> expression. Following the initial experiment, cells were grown to confluency and plated in a 12-well plate at 20,000 cells/well with 1mL/well. Control and SHSY5YDiff cells were treated over a 6-day period as previously mentioned, with an additional media change on day 6, 24hrs before harvest. A third treatment group was grown in the same respect as SHSY5YDiff cells with an additional 24hr 1uM DX308 cDMEM media treatment (Table 3.1, Figure 3.1, Exp. 2, Figure 3.6). It should be noted that this media only contained 1uM DX308 cDMEM media without TPA.

### 3.2.3 Differential Gene Expression

#### 3.2.3.1 RNA Isolation

After respective treatment times cells were harvested using the Qiagen RNeasy® Mini Kit (Qiagen, 74106). Supernatant was collected and centrifuged for later investigations. Cells were lysed using 600uL of RLT lysis buffer (Qiagen, 1015762) in their 12-well plates for 5 minutes



on a plate shaker. Cell lysate was then mixed with equal part 70% EtOH/ 30% DEPC H<sub>2</sub>O (Ethanol: Deacon Labs, 3961EA) (DEPC H<sub>2</sub>O: Fisher BioReagents, BP561-1). The lysate ethanol cell mix was then loaded and washed on a RNeasy spin column (Qiagen, 1112543) with RW1 (Qiagen, 1015763) and RPE (Qiagen, 1018013) wash buffers used respectively. Finally, the column was eluted with 40uL of DEPC H<sub>2</sub>O in a clean collection tube (Qiagen, 1017981). Purified RNA was stored in -20°C freezer until reverse transcription can be performed.

### 3.2.3.2 RT-qPCR

Purity and concentration of isolated RNA was measured using NanoDrop 2000c (Thermo Scientific). cDNA microtubes (Thermo Scientific, AB-0784) were loaded with DEPC H<sub>2</sub>O (Fisher BioReagents, BP561-1), purified RNA, and an iScript cDNA Synthesis Kit (Bio-Rad, 1708891). The iScript Kit mix comprised of 5x iScript reaction mix (1708889) and iScript Reverse Transcriptase (LOO7877B), with 4uL and 1uL per cDNA microtube respectively. RNA concentration was normalized to 25ng/uL with V<sub>f</sub>=20uL prior to reverse transcription, 500ng total. After loading, cDNA tubes were moved into a thermocycler (Bio-Rad, MyCycler™ Version 1.065) for reverse transcription. Following an iScript protocol (activation: 5min/25°C, 20min/46°C, 1min/95°C, hold/4°C) for reverse transcription. After reverse transcription cDNA was kept at -20°C in a freezer until qPCR can be performed.

**Table 3.2: Primer List.** Target genes of interest used for all cell culture experiments.

Gene Name	NCBI: ID#	IDT: Assay ID#	Ref. Seq. Accession #
36B4	6175	Hs.PT.58.20222060	NM_053275
CYP26A1	1592	Hs.PT.58.2905296	NM_000783(2)
CYP26B1	56603	Hs.PT.58.38517191	NM_019885(1)
RAR $\alpha$	5914	Hs.PT.58.3892911	NM_000964(3)
RAR $\beta$	5915	Hs.PT.58.364456	NM_000965(2)
RAR $\gamma$	5916	Hs.PT.58.20057995	NM_001243731(2)
CRABP2	1382	Hs.PT.58.988113	NM_004164(1)
DRD1	1812	Hs.PT.58.1250643.gs	NM_000794(1)
DRD2	1813	Hs.PT.58.39162160	NM_000795(2)
DRD3	1814	Hs.PT.58.38968613	NM_000796(2)

For qPCR the cDNA was diluted 1:2 with DEPC H<sub>2</sub>O for a final concentration of 12.5ng/uL. A total of 2uL of cDNA, 25ng/well, was pipetted into the respective well following biological treatment group. 8uL of a SYBR Green master mix was then pipetted into respective target wells, according to the target gene of interest. SYBR Green master mix comprised of 5uL PerfeCTa® SYBR® GreenFastMix® (QuantaBio, 84069), 1uL target primer (Table 3.2), and 2uL DEPC H<sub>2</sub>O per reaction well. All qPCR experiments used 36B4 (RPLP0) as reference gene and were plated on a 384 well qPCR plate (Bio-Rad, HSP3805) in technical duplicates. When all wells were loaded the plate was centrifuged and placed in CFX384™ Real-Time System C1000

Touch™ ThermalCycler (Bio-Rad, 1855484) for qPCR analysis. SYBR Green qPCR analysis protocol, labeled SYBER BioRad (activation: 2min/95°C, 40 cycles: 5sec/95°C, 30sec/60°C, plate read; 31sec/65°C, 5sec/65°C) was performed for all experiments.

qPCR data was analyzed using Bio-Rad CFX Maestro for Mac 1.0 (Bio-Rad, Version 4.0.2325.0418). Wells were excluded if their melt curves show a primer dimer formation observed as a double peak within the melt curve, or if Cq value was not available due to faulty loading. Wells were grouped by biological treatments and target gene, with expression change normalized to the reference gene and relative to control,  $\Delta\Delta Cq$  and 36B4 respectively. Statistical significance of expression for biological group vs multiple groups analysis was done by a one-way ANOVA with Tukey corrections for multiple comparisons. Raw Cq values were extracted from CFX Maestro software and analyzed in GraphPad Prism 8.

### 3.3 Results

#### 3.3.1 atRA response in SNB19 & SHSY5Y cells

Preliminary experiments with both cell lines investigated expression of genes associated with atRA metabolism (CYP26A1/B1, CRABP2, RAR $_{\alpha,\beta,\gamma}$ ), and the effect of atRA treatments with comparisons of atRA/RAMBA (DX308) co-treatments. These experiments had the intended purpose of observing an atRA response previously mentioned in section 3.1 across both cell lines with a comparable increased response upon DX308 co-treatment.

The first experiment revealed that all genes of interest were expressed in SNB19 cells. An atRA response was observed as significant increase in CYP26A1 expression. Our results show a dose dependent increase in atRA response as seen by the significantly

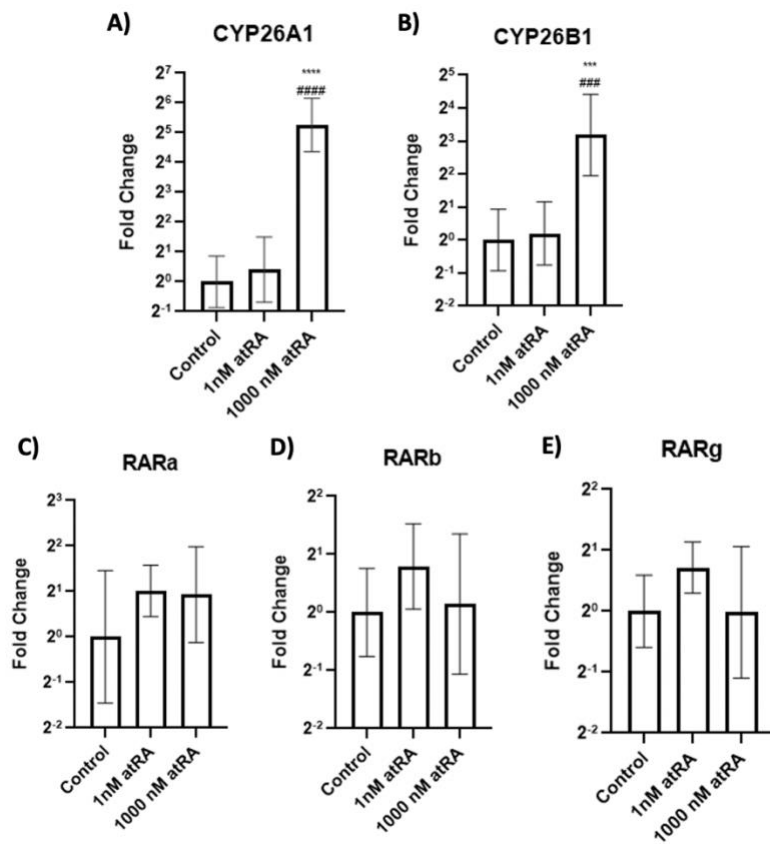


**Figure 3.2: JML\_101-SNB19 atRA Treatment.** Gene expression of CYP26A1/B1 and RARs in presence of 1uM atRA, and 1nM atRA. 0.1% DMSO used as control. A/B) CYP26A1/B1 gene expression. C/D/E) Target RARs gene expression alone for scale. Cell culture treatments run in biological triplicates, qPCR carried out in technical duplicates. Significance determined through  $\Delta\Delta Cq$  one-way ANOVA with Tukey corrections for multiple comparisons. (\* vs Control, # vs 1nM atRA) (\*\*\*) $p < 0.001$ .

increased expression between 1nM and 1uM atRA. All retinoic acid receptors do not show a significant increase in expression relative to control under 1nM or 1uM atRA treatment. The standard error of mean was relatively large across all target groups due to varied double peaks in melt curves. The initial pipetting technique was faulty for <4% of the wells during qPCR plating (Figure 3.2).

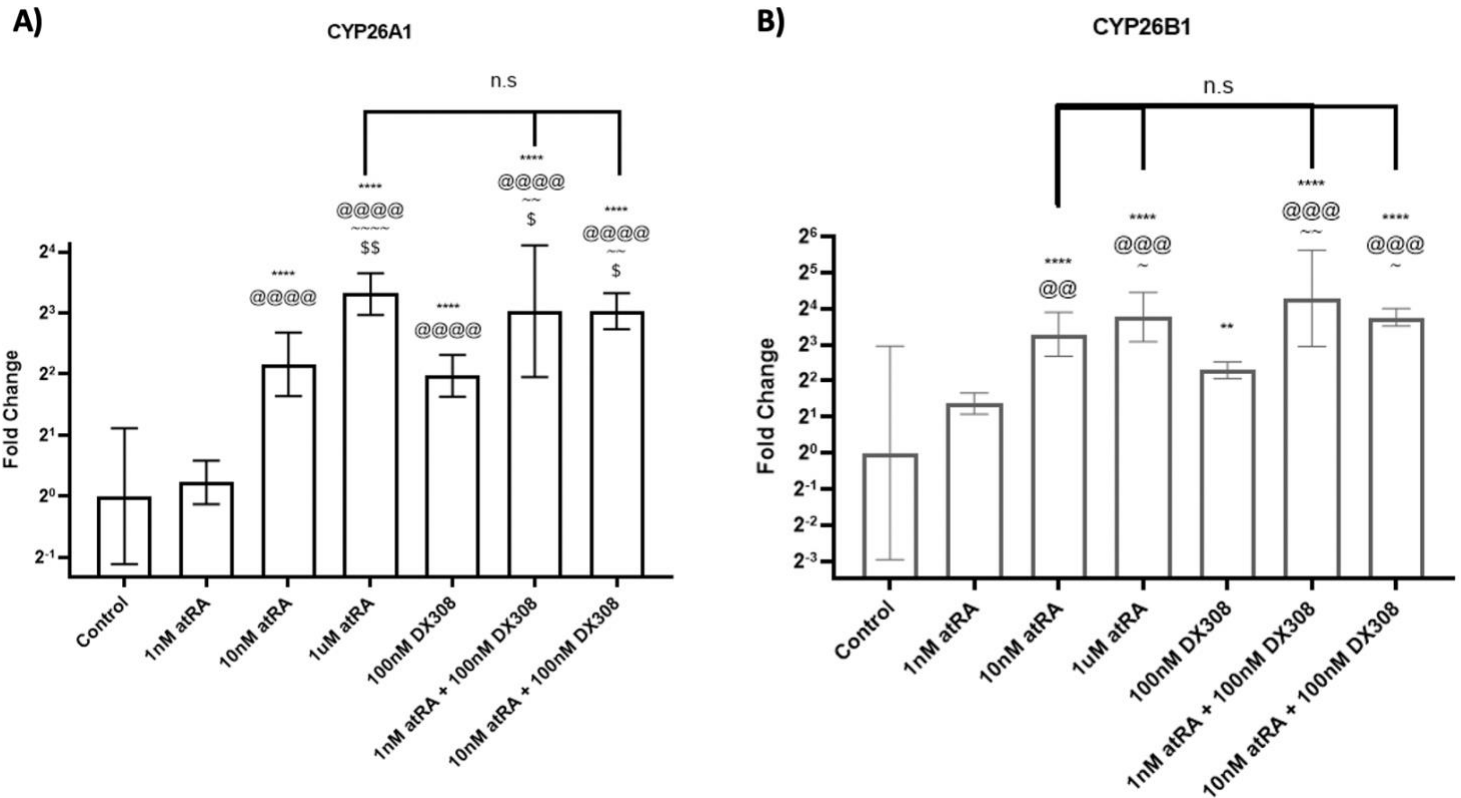


**Figure 3.3: JML\_111-SNB19-atRA/DX308.** Repeated SNB19 atRA response treatments with added DX308 solo and co-atRA treatments. A) CYP26A1 gene expression. B) CYP26B1 gene expression. Cell culture treatments run in biological triplicates; qPCR carried out in technical duplicates. Significance determined through  $\Delta\Delta Cq$  one-way ANOVA with Tukey corrections for multiple comparisons. (\* vs control, @ vs 1nM atRA, ~ vs 10nM atRA, \$ vs 100nM DX308) (\* $p < 0.05$ , \*\* $p < 0.01$ , \*\*\* $p < 0.001$ , \*\*\*\* $p < 0.0001$ ).

In the follow up SNB19 experiment we can see transcription of CYP26A1 again have significant increase in expression when compared to lower doses and the control (10nM: 1uM). There was also significant increase in atRA signaling when lower doses of atRA were combined with low doses of DX308 CYP26A1/B1 inhibitor. We can see this by comparing 10nM atRA/100nM DX308 co-treatment with 1uM atRA solo treatment. The increased expression of CYP26A1 and CYP26B1 as a factor of atRA response is similar between these combined and solo treatments. Because there is a significant difference between the solo atRA and co-DX308 treatments DX308 exhibits the necessary response for a viable RAMBA. Taken together this

supports inhibition of atRA metabolism via DX308's action on CYP26A1/B1 enzyme, observed as an increased atRA response under lower atRA concentrations. Additionally we observed direct expression of RAR $_{\alpha,\beta,\gamma}$  in the SNB19 cells; while not significant this does allow for atRA directed transcription of RARE (Figure 3.3).

In the initial experiment with the SHSY5Y cell line all genes of interest were expressed in the neuroblastoma immature undifferentiated state. Additionally, we observed a dose dependent atRA response with 100nM and 10nM atRA treatment. Combined treatments of respective atRA concentrations with 1uM DX308 do not have significant expression of CYP26A1 relative to the solo atRA treatment. This indicates that DX308 is not potentiating the atRA response. Data also supports previous investigations by Armstrong et al. 2007 where atRA treatments produce an increased atRA response relative to control. Importantly SHSY5Y cells express CYP26A1, and the respective gene can act as atRA response marker in this cell line. In addition to atRA response, RAR $_{\beta}$  is also expressed within the cell line. This is important as future investigations will target genes associated with Parkinson's and RAR $_{\beta}$  promotor sights (Niewiadomska-Cimicka et al., 2017). DRD2 and CRABP2 is expressed at low levels for all treatment groups (Supplemental Data). It is hypothesized that differentiated SHSY5Y cells will have significant increase in DRD expression relative to immature "control" SHSY5Y cells. Note that column 2 control wells in RT-qPCR are excluded due to Cq values >2 cycles off biological group. This was caused by problems with low cDNA concentration prior to pipetting in the 384 well plate, the corresponding cDNA tube was incorrectly loaded for reverse transcription (jFigure 3.4).

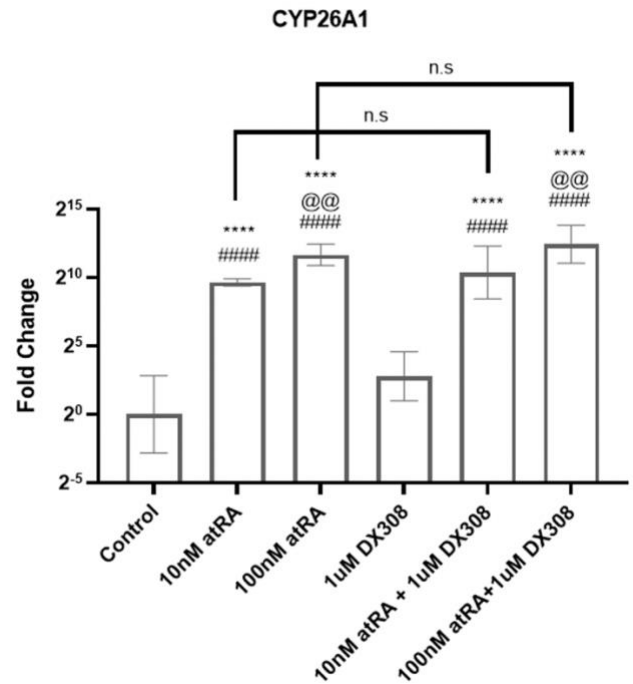


**Figure 3.4: JML\_127-SHSY5Y-atRA/DX308.** Initial SHSY5Y cell culture investigation for atRA response. CYP26A1 gene expression. Cell culture treatments run in biological triplicates; qPCR carried out in technical duplicates. Significance determined through  $\Delta\Delta Cq$  one-way ANOVA with Tukey corrections for multiple comparisons.) (\* vs control, # vs 1uM DX308, @ vs 10nM atRA) (\*\*p<0.01, \*\*\*p<0.001.)

### 3.3.2 atRA/TPA Differentiation of SHSY5Y Cells Effect on Dopamine Receptor

The specific purpose of the dopaminergic differentiated SHSY5Y experiments was: first, to observe SHSY5Y cells increase expression of DRD receptors relative to immature (control) SHSY5Y cells, and second; that we can use the differentiated SHSY5Y cells as a dopaminergic neuronal model for future DX308 treatments (Figure 3.1).

In the first experiment we observe a significant increase in CYP26A1 transcription in the atRA/TPA treatment group. This suggests that atRA could still be in the system at time of harvest, or we are observing prolonged 72hr atRA signaling from the initial 10uM atRA treatment (Day 0-3). The follow up experiment, jml\_141, reveals a possible TPA induced CYP26A1 transcription. While DRD2 receptor does not have significant increase in transcription under atRA/TPA treatment we do observe a slight increase in expression. This is also observed in RAR $\beta$  expression and allows the possibility for atRA targeted transcription of RARE described above. Overall, we see atRA signaling on day 7 of atRA/TPA differentiated SHSY5Y cells; however, the means of induction cannot be precisely attributed to the presence of atRA. Additionally, the atRA/TPA treatment group expressed DRD receptors slightly higher than control suggesting that some differentiation

was taking place. It should be noted that all column 2 control wells were excluded due to problems in the culture well where over confluency lead to apoptosis of the entire well population and resulted in faulty mRNA at time of harvest. The second study avoided this over confluency issue by seeding the plates at 20,000 cells/well instead of 100,000 cells/well. At the time of harvest the wells were 70-80% confluent in jml\_141.

The second experiment with SHSY5YDiff cells supported jml\_135, where we again see an increase in CYP26A1 expression. Interestingly, DRD1 expression is significantly increased while the DRD2 expression is significantly decreased within the atRA/TPA treatment group.

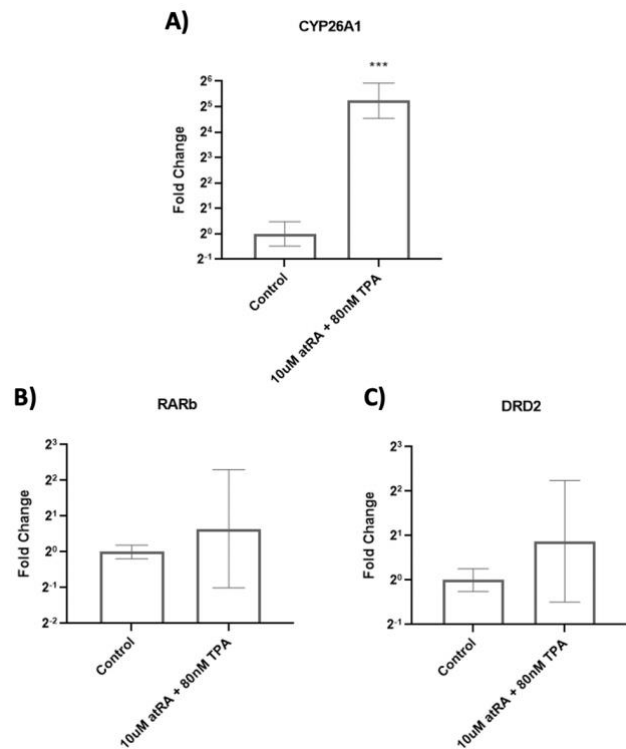


**Figure 3.5: JML\_135-SHSY5Y/SHSY5YDiff-atRA/TPA Regiment.** Secondary SHSY5Y cell culture experiment with interest on atRA/TPA induced dopaminergic differentiation. A) CYP26A1 gene expression. B) RARb gene expression. C) DRD2 gene expression. Cell culture treatments run in biological triplicates, qPCR carried out in technical duplicates. Significance determined through  $\Delta\Delta Cq$  one-way ANOVA with Tukey corrections for multiple comparisons. (\* vs control) (\*\*\*) p < 0.001

This expression profile is lost within the additional 24hr DX308 treatment group (Figure 3.6).

This indicates there is possible differentiation in treatment group 2 under terminal TPA stimulation, but seems to be lost with DX308 24hr treatment. A possible explanation for this is TPA induction of DRD receptor expression in addition to CYP26A1/B1. This is inferred due to the lack of TPA in the SHSY5YDiff\_DX308 treatment group 24hrs prior to harvest. Future experiments will have a TPA only treatment group to compare to current atRA/TPA differentiation model.

This data supports the previous experiment by having an atRA response in differentiated SHSY5Y cells; while being unable to shed light on the additional DX308 treatment within the context of an observable atRA response and DRD expression. DRD expression profile in atRA/TPA treatment group calls for further investigations on TPA directed differentiation. Future studies are needed to repeat this experiment. Taking special consideration for TPA differentiation, and additional DX308 treatments (Figure 3.6).

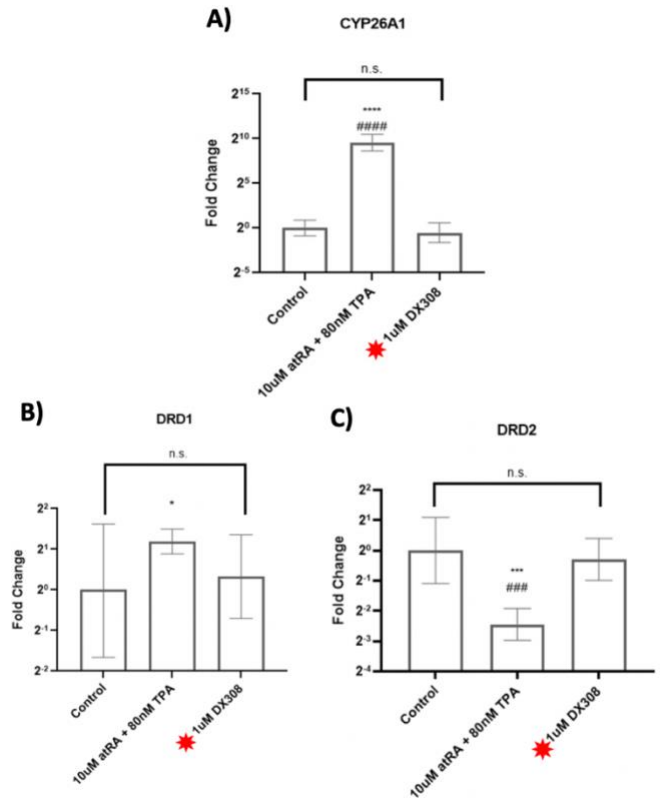


**Figure 3.6: JML\_141-SHSY5Y/SHSY5YDiff/SHSY5YDiffDX308.** Repeated atRA/TPA SHSY5Y cell culture experiment with additional 24hr DX308 biological treatment group (red star). A) CYP26A1 gene expression. B, C) Dopamine receptors gene expression. Cell culture treatments run in biological triplicates; qPCR carried out in technical duplicates. Significance determined through  $\Delta\Delta Cq$  one-way ANOVA with Tukey corrections for multiple comparisons) (\* vs control, # vs 1uM DX308) (\*\*\*)  $p < 0.001$ )

### 3.4 Discussion

The overarching goal of these experiments centered around preliminary *in vitro* modeling of gliosis after TBI and the death of dopaminergic neurons found in PD patients with the explicit purpose of guided atRA signaling as a mediator of pathogenesis. Importantly we used cost effective cell lines; either previously used in the Diaz lab, SHSY5Y, or donated by the Bridges lab, SNB19. SNB19 cells were selected with the intention of modeling a brain injury in a dish due to their ability to express GFAP as a marker of reactive gliosis (McMillian et al., 1994). SHSY5Y cells were selected due to their diverse ability of differentiation and substantial history as a model for PD (Xicoy et al., 2017).

The initial purpose of the experiments needed to prove that both cell lines expressed the primary target of novel RAMBA DX308, CYP26A1/B1. Additionally, for the rough models to be viable the cell lines also needed to express transport machinery, CRABP2, and atRA directed nuclear receptors,  $RAR_{\alpha,\beta,\gamma}$ . Observations of these genes expressed in the cell line would therefore allow for theoretical atRA guided transcription and subsequent metabolism for homeostatic signaling. We intended to induce targeted inhibition of CYP26A1/B1 in order to increase the endogenous levels of atRA and subsequent signaling. Overall our experiments were a success in this context. SNB19, SHSY5Y, and SHSY5YDiff all expressed the genes of interest pertaining to atRA metabolism and guided transcription. Unfortunately, SNB19 experiments did not successfully investigate CRABP2 expression; however, due to the presence of RARs atRA directed signaling is still supported in the cell line (Table 3.1, Figure 3.2, 3.3). The secondary purpose for all experiments needed to show an atRA response under atRA treatment and DX308 co-treatment. Successful inhibition of atRA clearance via DX308 would potentiate the atRA response under low doses of atRA co-treatment compared to same dose atRA solo treatment. With the acceptance of SHSY5YDiff\_DX308 treatment group (Figure 3.6, Group 3-red star) we observed a dose dependent atRA response across SNB19, SHSY5Y cell lines; and an atRA response within the SHSY5YDiff cell line. It should be noted that SHSY5YDiff cell line could have CYP26A1 expression mediated by terminal TPA treatment, and future experiments will investigate this possibility (Figure 3.5, Group 2). We suspect this due to the observed atRA response in jml\_135 in SHSY5YDiff, but the loss of this expression profile once DX308 is administered post differentiation regiment for 24hrs before harvest (Table 3.1, Figure 3.1-Exp.2). Importantly we observed a DX308 potentiated atRA response in the SNB19 cell lines with respect to solo atRA treatments (Figure 3.2, 3.3). This is important indicator for future studies surrounding gliosis and PD induced stress models as atRA could reduce the pathogenesis of both diseases.

Finally, this research attempted to differentiate SHSY5Y cell line into a dopaminergic neuronal culture following Presgraves et al., 2004 protocol. With respects to DRD expression, the atRA/TPA differentiation regiment exhibited an interesting expression profile that was not consistent across experiments. DRD1 had significant increase in expression only in one experiment while DRD2 had significant decrease in expression in only one experiment. Under an atRA/TPA regiment CYP26A1 expression seems to be increased, this effect is lost when the



final 24hr treatment is replaced with DX308 alone. Follow up experiments report an altered DRD expression between DRD1 and DRD2 when compared to the first experiment. Although these expression profiles suggest the possibility for differentiation under atRA/TPA regiment repeated SHSY5Y differentiation experiments must be preformed in order to draw more valid conclusions. (Figure 3.1, 3.4, 3.5). *In vitro* dopaminergic neurons are a closer model to PD and future studies will utilize the differentiation protocol in coordination with MPTP/MPP<sup>+</sup> cytotoxicity experiments to assess the viability of atRA mediated cell survival. These experiments are only preliminary investigations surrounding DX308's ability to inhibit atRA clearance for neuronal cell lines. Taken together this research has shown a rough model of glial, neuronal, and dopaminergic cell lines that can utilize atRA as a homeostatic signaling factor. At its basic level we can use this knowledge to investigate DX308 as a therapeutic drug in the CNS with the intention of increasing endogenous atRA following TBI or PD diagnosis.

## **4. Conclusion & Future Directions**

### **4.1 Conclusion**

These experiments establish a rough *in vitro* model for investigations surrounding atRA signaling and the pharmacological applications of RAMBAs. DX308 inhibition of atRA metabolism via CYP26A1/B1 unlocks the possibility for therapeutic intervention in TBI and PD. The role of RA signaling following CNS injury is emerging as a primary target for mediation of important neuronal genes needed to attenuate TBI and PD. Focusing on particular genes of interest under RAR guided transcription is a great place to expand in this area. For example: FGF9, BCL-x, NF-KB1, and CAMK2 $\alpha$  all have RAR $\beta$  binding sites and are expressed in either SNB19 or SHSY5Y cells (Hodges et al., 2006; Niewiadomska-Cimicka et al., 2017; Rouillard et al., 2016). This research was limited to specific cell line expression of atRA synthesis and transcription machinery in the CNS and provides the possibility for DX308 application as an atRA signaling activator. Activation of atRA signaling pathway following TBI is a major contributor to this ideology. The cytotoxicity surrounding the Ca<sup>2+</sup>/Glu cascade may be attenuated by non-canonical atRA signaling through dampening of MAPK activation. Significantly lowering Ca<sup>2+</sup> stress may halt mitochondrial and cell membrane mediated destruction, leading to neuronal survival. As we have seen in these experiments and reported in previous literature atRA also retains the ability to control differentiation of some neuronal populations. Altering active microglia states to favor M2 phagocytotic differentiation may be

under the influence of atRA signaling following TBI. Administration of atRA following TBI in mice show a neuroprotective effect and reduction in astrogliosis seven days after the injury. RA also has pervasive applications in altering PD pathology. Research previously found oral administration of RAR agonist prevented dopaminergic cell loss in the substantia nigra supporting the role of RA directed neuronal survival (Katsuki et al., 2009). Further evidence surrounds the role RA plays in dopaminergic differentiation and mediated expression of dopamine receptors. When considering the beneficial effects of atRA signaling in neurodegenerative diseases the therapeutic goal would be to endogenously control the intracellular concentrations. One way of increasing intracellular RA is to inhibit CYP26A1/B1 metabolism. Since DX308 is permeable to the BBB this drug could be administered intravenously to combat both TBI and PD. In this work we confirm our hypothesis that DX308 is a substrate-based CYP26A1 and B1 inhibitor which inhibit the degradation of atRA in CNS cell model and that this degradation is modulated by CYP26A1 and B1 which are expressed in these cells and have their expression increase after atRA treatment. Additional work is needed to fully demonstrate the therapeutic utility of DX308 on the treatment of neurodegenerative diseases but based on our preliminary experiments it represents a promising candidate for further in vitro and in vivo studies.

## 4.2 Future Directions

In the immediate realm of this research repeated RT-qPCR should be performed for all experiments in order to support these preliminary findings. Additionally, the intracellular carrier protein for retinoic acid directed transcription, CRABP2, should be added to the gene target list for the repeated experiments. Other target genes for SNB19 include: GFAP, FGF9, BCL-X, and EAAT1 (SLC1A3). These genes have either been found to be expressed in the specific cell line or have RAR $\beta$  binding sites for RA guided transcription (Rouillard et al., 2016; Niewiadomaska-Cimicka, 2017). GFAP is an important gene target as it can be considered a marker for gliosis in most astroglia cell lines (Verkhatsky et al., 2014). Another gene of interest for the SHSY5Y cell line is CAMK2 $\alpha$  which is expressed in the cell line and has RAR $\beta$  binding sites. NfKB1 also has RAR $\beta$  binding sites and should be added to the list of target genes for future investigations. These genes are useful as canonical and non-canonical signaling may lend supporting evidence for RA mediation of inflammation and excitotoxicity in TBI and PD pathology. Cell cultures would undergo similar protocols for RAMBA co-treatments with special interest on the

expression relationship relative to an observed atRA response. Other cell culture experiments that can end in RT-qPCR would revolve around cytotoxicity models and how they affect target gene transcription relative to atRA and DX308 co-treatments. SNB19 can be treated with LPS, ROS, and TNF $\alpha$  in tandem with atRA or DX308 co-treatments to model TBIs and therapeutic intervention with respect to the effects of atRA directed signaling. Special interest would consider the relationship between activated gliosis and atRA response by monitoring the expression of GFAP and CYP26A1/B1 respectively. SHSY5Y cells can undergo MPTP/MPP<sup>+</sup> treatments to model neurodegeneration similar to PD. The goal would be to observe how modeling PD in vitro with SHSY5YDiff would affect the atRA response and target genes associated with neuroinflammation and protection. In coordination with these RT-qPCR experiments ELISA assays would need to be performed in tandem with cell culture constraints. Under the same cytotoxicity/PD model and atRA/DX308 co-treatments ELISA antibodies would look for TNF $\alpha$ , IL-1 $\beta$ , and IL-6 as indicators of inflammation following cell culture treatments. Anti-inflammatory cytokines under investigation would include: IL-4, IL-10, BDNF $\alpha$ , and TGF- $\beta$ . Understanding the inflammatory signaling after modeling the neurovegetative disease in coordination with atRA/DX308 treatments would give tremendous insight on the possible neuroprotective effects of both atRA and the novel RAMBA, DX308. Together this research could be published as the discovery of a new RAMBA that can be used to diminish the 2<sup>o</sup> insult of TBIs or combat the pathogenesis of PD by alleviating the death of dopaminergic neurons. atRA has an important regulatory role in the central nervous system, unlocking the signaling effects of increased endogenous atRA as it pertains to TBI and PD could be the fundamental step in treating these neurodegenerative diseases.

## 5. References

- Abdul-Muneer PM, Chandra N, Haorah J (2015) Interactions of Oxidative Stress and Neurovascular Inflammation in the Pathogenesis of Traumatic Brain Injury. *Mol Neurobiol* 51:966–979.
- Adamson PC, Bailey J, Pluda J, Poplack DG, Bauza S, Murphy RF, Yarchoan R, Balis FM (1995) Pharmacokinetics of all-trans-retinoic acid administered on an intermittent schedule. *JCO* 13:1238–1241.
- Al Tanoury Z, Piskunov A, Andriamoratsiresy D, Gaouar S, Lutzinger R, Ye T, Jost B, Keime C, Rochette-Egly C (2013) Genes involved in cell adhesion and signaling: A new repertoire of Retinoic Acid Receptors target genes in mouse embryonic fibroblasts. *Journal of Cell Science:jcs*.131946.
- Armstrong JL, Taylor GA, Thomas HD, Boddy AV, Redfern CPF, Veal GJ (2007) Molecular targeting of retinoic acid metabolism in neuroblastoma: the role of the CYP26 inhibitor R116010 in vitro and in vivo. *Br J Cancer* 96:1675–1683.
- Armstrong MJ, Okun MS (2020) Diagnosis and Treatment of Parkinson Disease: A Review. *JAMA* 323:548.
- Bachstetter AD, Norris CM, Sompol P, Wilcock DM, Goulding D, Neltner JH, St. Clair D, Watterson DM, Van Eldik LJ (2012) Early Stage Drug Treatment That Normalizes Proinflammatory Cytokine Production Attenuates Synaptic Dysfunction in a Mouse Model That Exhibits Age-Dependent Progression of Alzheimer's Disease-Related Pathology. *Journal of Neuroscience* 32:10201–10210.
- Barone P, Poewe W, Albrecht S, Debieuvre C, Massey D, Rascol O, Tolosa E, Weintraub D (2010) Pramipexole for the treatment of depressive symptoms in patients with Parkinson's disease: a randomised, double-blind, placebo-controlled trial. *The Lancet Neurology* 9:573–580.
- Bastien J, Rochette-Egly C (2004) Nuclear retinoid receptors and the transcription of retinoid-target genes. *Gene* 328:1–16.
- Batchelor P (2002) Macrophages and Microglia Produce Local Trophic Gradients That Stimulate Axonal Sprouting Toward but Not beyond the Wound Edge. *Molecular and Cellular Neuroscience* 21:436–453.
- Böttner M, Zorenkov D, Hellwig I, Barrenschee M, Harde J, Fricke T, Deuschl G, Egberts J-H, Becker T, Fritscher-Ravens A, Arlt A, Wedel T (2012) Expression pattern and localization of alpha-synuclein in the human enteric nervous system. *Neurobiology of Disease* 48:474–480.

- Braak H, Tredici KD, Rüb U, de Vos RAI, Jansen Steur ENH, Braak E (2003) Staging of brain pathology related to sporadic Parkinson's disease. *Neurobiology of Aging* 24:197–211.
- Brochard V, Combadière B, Prigent A, Laouar Y, Perrin A, Beray-Berthet V, Bonduelle O, Alvarez-Fischer D, Callebert J, Launay J-M, Duyckaerts C, Flavell RA, Hirsch EC, Hunot S (2008) Infiltration of CD4+ lymphocytes into the brain contributes to neurodegeneration in a mouse model of Parkinson disease. *J Clin Invest*: JCI36470.
- Chandra V, Wu D, Li S, Potluri N, Kim Y, Rastinejad F (2017) The quaternary architecture of RAR $\beta$ -RXR $\alpha$  heterodimer facilitates domain-domain signal transmission. *Nat Commun* 8:868.
- Chen Y, Huang L, Solursh M (1994) A Concentration Gradient of Retinoids in the Early *Xenopus laevis* Embryo. *Developmental Biology* 161:70–76.
- Cheng G, Kong R, Zhang L, Zhang J (2012) Mitochondria in traumatic brain injury and mitochondrial-targeted multipotential therapeutic strategies: Mitochondria in traumatic brain injury. *British Journal of Pharmacology* 167:699–719.
- Chiang M-Y, Misner D, Kempermann G, Schikorski T, Giguère V, Sucov HM, Gage FH, Stevens CF, Evans RM (1998) An Essential Role for Retinoid Receptors RAR $\beta$  and RXR $\gamma$  In Long-Term Potentiation and Depression. *Neuron* 21:1353–1361.
- Cohlan SQ (1953) Excessive Intake of Vitamin A as a Cause of Congenital Anomalies in the Rat. *Science* 117:535–536.
- Cookson MR (2012) Cellular effects of LRRK2 mutations. *Biochemical Society Transactions* 40:1070–1073.
- Cornelius C, Crupi R, Calabrese V, Graziano A, Milone P, Pennisi G, Radak Z, Calabrese EJ, Cuzzocrea S (2013) Traumatic Brain Injury: Oxidative Stress and Neuroprotection. *Antioxidants & Redox Signaling* 19:836–853.
- Corti O, Lesage S, Brice A (2011) What Genetics Tells us About the Causes and Mechanisms of Parkinson's Disease. *Physiological Reviews* 91:1161–1218.
- D'Ambrosio, D.N.; Clugston, R.D.; Blaner, W.S. Vitamin A Metabolism: An Update. *Nutrients* 2011, 3, 63-103.
- Delacroix L, Moutier E, Altobelli G, Legras S, Poch O, Choukrallah M-A, Bertin I, Jost B, Davidson I (2010) Cell-Specific Interaction of Retinoic Acid Receptors with Target Genes in Mouse Embryonic Fibroblasts and Embryonic Stem Cells. *Mol Cell Biol* 30:231–244.
- Devine MJ, Gwinn K, Singleton A, Hardy J (2011) Parkinson's disease and  $\alpha$ -synuclein expression. *Mov Disord* 26:2160–2168.

- Driver JA, Logroscino G, Gaziano JM, Kurth T (2009) Incidence and remaining lifetime risk of Parkinson disease in advanced age. *Neurology* 72:432–438.
- Dugger BN, Dickson DW (2017) Pathology of Neurodegenerative Diseases. *Cold Spring Harb Perspect Biol* 9:28-35.
- Dumetz F, Buré C, Alfos S, Bonneu M, Richard E, Touyarot K, Marie A, Schmitter J-M, Bosch-Bouju C, Pallet V (2020) Normalization of hippocampal retinoic acid level corrects age-related memory deficits in rats. *Neurobiology of Aging* 85:1–10.
- Durmaz R, Kanbak G, Akyüz F, Isiksoy S, Yücel F, Inal M, Tel E (2003) Lazaroid Attenuates Edema by Stabilizing ATPase in the Traumatized Rat Brain. *Can j neurol sci* 30:143–149.
- El Hayek S, Allouch F, Razafsha M, Talih F, Gold MS, Wang KK, Kobeissy F (2020) Traumatic brain injury and methamphetamine: A double-hit neurological insult. *Journal of the Neurological Sciences* 411:116711.
- Fang Y, Liu H-X, Zhang N, Guo GL, Wan Y-JY, Fang J (2013) NURBS: a database of experimental and predicted nuclear receptor binding sites of mouse. *Bioinformatics* 29:295–297.
- Foti RS, Diaz P, Douguet D (2016b) Comparison of the ligand binding site of CYP2C8 with CYP26A1 and CYP26B1: a structural basis for the identification of new inhibitors of the retinoic acid hydroxylases. *Journal of Enzyme Inhibition and Medicinal Chemistry* 31:148–161.
- Foti RS, Isoherranen N, Zelter A, Dickmann LJ, Buttrick BR, Diaz P, Douguet D (2016a) Identification of Tazarotenic Acid as the First Xenobiotic Substrate of Human Retinoic Acid Hydroxylase CYP26A1 and CYP26B1. *Journal of Pharmacology and Experimental Therapeutics* 357:281–292.
- Fowler SC, Zarccone TJ, Vorontsova E, Chen R (2002) Motor and associative deficits in D2 dopamine receptor knockout mice. *Int j dev neurosci* 20:309–321.
- Fox SH, Katzenschlager R, Lim S-Y, Ravina B, Seppi K, Coelho M, Poewe W, Rascol O, Goetz CG, Sampaio C (2011) The Movement Disorder Society Evidence-Based Medicine Review Update: Treatments for the motor symptoms of Parkinson’s disease. *Mov Disord* 26:S2–S41.
- Franco PG, Paganelli AR, Lopez SL, Carrasco AE (1999) Functional association of retinoic acid and hedgehog signaling in *Xenopus* primary neurogenesis. *Development* 126:4257–4265.
- Galgano M, Toshkezi G, Qiu X, Russell T, Chin L, Zhao L-R (2017) Traumatic Brain Injury: Current Treatment Strategies and Future Endeavors. *Cell Transplant* 26:1118–1130.

- Galgano M, Toshkezi G, Qiu X, Russell T, Chin L, Zhao L-R (2017) Traumatic Brain Injury: Current Treatment Strategies and Future Endeavors. *Cell Transplant* 26:1118–1130.
- Gao L (2016) Traumatic brain injury a review of characteristics molecular basis and management. *Front Biosci* 21:890–899.
- Germain P, Chambon P, Eichele G, Evans RM, Lazar MA, Leid M, De Lera AR, Lotan R, Mangelsdorf DJ, Gronemeyer H (2006a) International Union of Pharmacology. LX. Retinoic Acid Receptors. *Pharmacol Rev* 58:712–725.
- Germain P, Chambon P, Eichele G, Evans RM, Lazar MA, Leid M, De Lera AR, Lotan R, Mangelsdorf DJ, Gronemeyer H (2006b) International Union of Pharmacology. LXIII. Retinoid X Receptors. *Pharmacol Rev* 58:760–772.
- Goldman JG, Guerra CM (2020) Treatment of Nonmotor Symptoms Associated with Parkinson Disease. *Neurologic Clinics* 38:269–292.
- Goodman, A. B., & Pardee, A. B. (2003). Evidence for defective retinoid transport and function in late onset Alzheimer's disease. *Proceedings of the National Academy of Sciences*, 100(5), 2901–2905.
- Gronemeyer H, Gustafsson J-Å, Laudet V (2004) Principles for modulation of the nuclear receptor superfamily. *Nat Rev Drug Discov* 3:950–964.
- Hale F (1933) Pigs Born without Eye Balls. In: *Problems of Birth Defects* (Persaud TVN, ed), pp 166–167.
- Halestrap AP (2009) What is the mitochondrial permeability transition pore? *Journal of Molecular and Cellular Cardiology* 46:821–831.
- Harris JP, Burrell JC, Struzyna LA, Chen HI, Serruya MD, Wolf JA, Duda JE, Cullen DK (2020) Emerging regenerative medicine and tissue engineering strategies for Parkinson's disease. *npj Parkinsons Dis* 6:4.
- Hayes DP (2007) Nutritional hormesis. *Eur J Clin Nutr* 61:147–159.
- Heinzel T, Lavinsky RM, Mullen T-M, Söderström M, Laherty CD, Torchia J, Yang W-M, Brard G, Ngo SD, Davie JR, Seto E, Eisenman RN, Rose DW, Glass CK, Rosenfeld MG (1997) A complex containing N-CoR, mSin3 and histone deacetylase mediates transcriptional repression. *Nature* 387:43–48.
- Hernandez-Ontiveros DG, Tajiri N, Acosta S, Giunta B, Tan J, Borlongan CV (2013) Microglia Activation as a Biomarker for Traumatic Brain Injury. *Front Neurol* 4.

- Hinzman JM, Wilson JA, Mazzeo AT, Bullock MR, Hartings JA (2016) Excitotoxicity and Metabolic Crisis Are Associated with Spreading Depolarizations in Severe Traumatic Brain Injury Patients. *Journal of Neurotrauma* 33:1775–1783.
- Hodges A et al. (2006) Regional and cellular gene expression changes in human Huntington's disease brain. *Human Molecular Genetics* 15:965–977.
- Hummel R, Ulbrich S, Appel D, Li S, Hirnet T, Zander S, Bobkiewicz W, Gözl C, Schäfer MKE (2020) Administration of all- *trans* retinoic acid after experimental traumatic brain injury is brain protective. *Br J Pharmacol* 177:5208–5223.
- Iñiguez MA, Morte B, Rodriguez-Peña A, Muñoz A, Gerendasy D, Sutcliffe JG, Bernal J (1994) Characterization of the promoter region and flanking sequences of the neuron-specific gene RC3 (neurogranin). *Molecular Brain Research* 27:205–214.
- International Parkinson's Disease Genomics Consortium (IPDGC) et al. (2014) Large-scale meta-analysis of genome-wide association data identifies six new risk loci for Parkinson's disease. *Nat Genet* 46:989–993.
- Jenkins CL, Bretscher LE, Guzei IA, Raines RT (2003) Effect of 3-Hydroxyproline Residues on Collagen Stability. *J Am Chem Soc* 125:6422–6427.
- Jing J, Isoherranen N, Robinson-Cohen C, Petrie I, Kestenbaum B, Yeung C (2016) Chronic Kidney Disease Alters Vitamin A Homeostasis via Effects on Hepatic RBP4 Protein Expression and Metabolic Enzymes. *Clinical And Translational Science* 9:207–215.
- Katsuki H, Kurimoto E, Takemori S, Kurauchi Y, Hisatsune A, Isohama Y, Izumi Y, Kume T, Shudo K, Akaike A (2009) Retinoic acid receptor stimulation protects midbrain dopaminergic neurons from inflammatory degeneration via BDNF-mediated signaling. *Journal of Neurochemistry* 110:707–718.
- Kirschner PB, Jenkins BG, Schulz JB, Finkelstein SP, Matthews RT, Rosen BR, Flint Beal M (1996) NGF, BDNF and NT-5, but not NT-3 protect against MPP+ toxicity and oxidative stress in neonatal animals. *Brain Research* 713:178–185.
- Kopf E, Plassat J-L, Vivat V, de Thé H, Chambon P, Rochette-Egly C (2000) Dimerization with Retinoid X Receptors and Phosphorylation Modulate the Retinoic Acid-induced Degradation of Retinoic Acid Receptors  $\alpha$  and  $\gamma$  through the Ubiquitin-Proteasome Pathway. *Journal of Biological Chemistry* 275:33280–33288.
- Kovalevich J, Langford D (2013) Considerations for the Use of SH-SY5Y Neuroblastoma Cells in Neurobiology. In: *Neuronal Cell Culture* (Amini S, White MK, eds), pp 9–21 *Methods in Molecular Biology*. Totowa, NJ: Humana Press.
- Krežel W, Kastner P, Chambon P (1999) Differential expression of retinoid receptors in the adult mouse central nervous system. *Neuroscience* 89:1291–1300.



- Kumar A, Alvarez-Croda D-M, Stoica BA, Faden AI, Loane DJ (2016) Microglial/Macrophage Polarization Dynamics following Traumatic Brain Injury. *Journal of Neurotrauma* 33:1732–1750.
- Kumar A, Loane DJ (2012) Neuroinflammation after traumatic brain injury: Opportunities for therapeutic intervention. *Brain, Behavior, and Immunity* 26:1191–1201.
- Ladak AA, Enam SA, Ibrahim MT (2019) A Review of the Molecular Mechanisms of Traumatic Brain Injury. *World Neurosurgery* 131:126–132.
- le Maire A, Germain P, Bourguet W (2020) Protein-protein interactions in the regulation of RAR–RXR heterodimers transcriptional activity. In: *Methods in Enzymology*, pp 175–207. Elsevier.
- le Maire A, Teyssier C, Erb C, Grimaldi M, Alvarez S, de Lera AR, Balaguer P, Gronemeyer H, Royer CA, Germain P, Bourguet W (2010) A unique secondary-structure switch controls constitutive gene repression by retinoic acid receptor. *Nat Struct Mol Biol* 17:801–807.
- Liu Z, Wang X, Yu Y, Li X, Wang T, Jiang H, Ren Q, Jiao Y, Sawa A, Moran T, Ross CA, Montell C, Smith WW (2008) A Drosophila model for LRRK2-linked parkinsonism. *Proceedings of the National Academy of Sciences* 105:2693–2698.
- Long-Smith CM, Sullivan AM, Nolan YM (2009) The influence of microglia on the pathogenesis of Parkinson’s disease. *Progress in Neurobiology* 89:277–287.
- Lorente L (2017) Biomarkers Associated with the Outcome of Traumatic Brain Injury Patients. *Brain Sciences* 7:142.
- Maden M (2002) Retinoid signalling in the development of the central nervous system. *Nat Rev Neurosci* 3:843–853.
- Mahony S, Mazzoni EO, McCuine S, Young RA, Wichterle H, Gifford DK (2011) Ligand-dependent dynamics of retinoic acid receptor binding during early neurogenesis. *Genome Biol* 12:R2.
- Marras C, Beck JC, Bower JH, Roberts E, Ritz B, Ross GW, Abbott RD, Savica R, Van Den Eeden SK, Willis AW, Tanner C (2018) Prevalence of Parkinson’s disease across North America. *npj Parkinson’s Disease* 4:21.
- Martens JHA, Brinkman AB, Simmer F, Francoijs K-J, Nebbioso A, Ferrara F, Altucci L, Stunnenberg HG (2010) PML-RAR $\alpha$ /RXR Alters the Epigenetic Landscape in Acute Promyelocytic Leukemia. *Cancer Cell* 17:173–185.

- McCaffery P, Drager UC (1994) High levels of a retinoic acid-generating dehydrogenase in the meso-telencephalic dopamine system. *Proceedings of the National Academy of Sciences* 91:7772–7776.
- McCoy MK, Cookson MR (2012) Mitochondrial Quality Control and Dynamics in Parkinson's Disease. *Antioxidants & Redox Signaling* 16:869–882.
- McMillian MK, Thai L, Hong J-S, O'Callaghan JP, Pennypacker KR (1994) Brain injury in a dish: a model for reactive gliosis. *Trends in Neurosciences* 17:138–142.
- Mendoza-Parra MA, Walia M, Sankar M, Gronemeyer H (2011) Dissecting the retinoid-induced differentiation of F9 embryonal stem cells by integrative genomics. *Mol Syst Biol* 7:538.
- Mey J (2006) New therapeutic target for CNS injury? The role of retinoic acid signaling after nerve lesions. *J Neurobiol* 66:757–779.
- Mey J, Mccaffery P (2004) Retinoic Acid Signaling in the Nervous System of Adult Vertebrates. *Neuroscientist* 10:409–421.
- Mioni G, Grondin S, Stablum F (2014) Temporal dysfunction in traumatic brain injury patients: primary or secondary impairment? *Front Hum Neurosci* 8.
- Morrow SE, Pearson M (2010) Management Strategies for Severe Closed Head Injuries in Children. *Seminars in Pediatric Surgery* 19:279–285.
- Moutier E, Ye T, Choukrallah M-A, Urban S, Osz J, Chatagnon A, Delacroix L, Langer D, Rochel N, Moras D, Benoit G, Davidson I (2012) Retinoic Acid Receptors Recognize the Mouse Genome through Binding Elements with Diverse Spacing and Topology. *Journal of Biological Chemistry* 287:26328–26341.
- Mustafa AG, Singh IN, Wang J, Carrico KM, Hall ED (2010) Mitochondrial protection after traumatic brain injury by scavenging lipid peroxyl radicals: TBI, mitochondria and lipid peroxidation. *Journal of Neurochemistry* 114:271–280
- Nagy L, Kao H-Y, Chakravarti D, Lin RJ, Hassig CA, Ayer DE, Schreiber SL, Evans RM (1997) Nuclear Receptor Repression Mediated by a Complex Containing SMRT, mSin3A, and Histone Deacetylase. *Cell* 89:373–380.
- Napoli JL (2017) Cellular retinoid binding-proteins, CRBP, CRABP, FABP5: Effects on retinoid metabolism, function and related diseases. *Pharmacology & Therapeutics* 173:19–33.
- Napoli JL (2020) Post-natal all-trans-retinoic acid biosynthesis. In: *Methods in Enzymology*, pp 27–54.
- Niewiadomska-Cimicka A, Krzyżosiak A, Ye T, Podleśny-Drabiniok A, Dembélé D, Dollé P, Krężel W (2017) Genome-wide Analysis of RAR $\beta$  Transcriptional Targets in Mouse

Striatum Links Retinoic Acid Signaling with Huntington's Disease and Other Neurodegenerative Disorders. *Mol Neurobiol* 54:3859–3878.

Noyce AJ, Bestwick JP, Silveira-Moriyama L, Hawkes CH, Giovannoni G, Lees AJ, Schrag A (2012) Meta-analysis of early nonmotor features and risk factors for Parkinson disease. *Ann Neurol* 72:893–901.

Obeso JA et al. (2017) Past, present, and future of Parkinson's disease: A special essay on the 200th Anniversary of the Shaking Palsy: The Shaking Palsy: Past, Present and Future. *Mov Disord* 32:1264–1310.

Ozelius LJ, Senthil G, Saunders-Pullman R, Ohmann E, Deligtisch A, Tagliati M, Hunt AL, Klein C, Henick B, Hailpern SM, Lipton RB, Soto-Valencia J, Risch N, Bressman SB (2006) *LRRK2* G2019S as a Cause of Parkinson's Disease in Ashkenazi Jews. *N Engl J Med* 354:424–425.

Park SW, Nhieu J, Persaud SD, Miller MC, Xia Y, Lin Y-W, Lin Y-L, Kagechika H, Mayo KH, Wei L-N (2019a) A new regulatory mechanism for Raf kinase activation, retinoic acid-bound Crabp1. *Sci Rep* 9:10929.

Park SW, Nhieu J, Lin Y-W, Wei L-N (2019b) All-trans retinoic acid attenuates isoproterenol-induced cardiac dysfunction through Crabp1 to dampen CaMKII activation. *European Journal of Pharmacology* 858:172485.

Penvose A, Keenan JL, Bray D, Ramlall V, Siggers T (2019) Comprehensive study of nuclear receptor DNA binding provides a revised framework for understanding receptor specificity. *Nat Commun* 10:2514.

Pohl E, Tomlinson CWE (2020) Classical pathways of gene regulation by retinoids. In: *Methods in Enzymology*, pp 151–173.

Polymeropoulos MH (1997) Mutation in the  $\alpha$ -Synuclein Gene Identified in Families with Parkinson's Disease. *Science* 276:2045–2047.

Power JHT, Barnes OL, Chegini F (2017) Lewy Bodies and the Mechanisms of Neuronal Cell Death in Parkinson's Disease and Dementia with Lewy Bodies: Lewy Bodies in Parkinson's Disease and Dementia with Lewy Bodies. *Brain Pathology* 27:3–12.

Presgraves SP, Ahmed T, Borwege S, Joyce JN (2003) Terminally differentiated SH-SY5Y cells provide a model system for studying neuroprotective effects of dopamine agonists. *Neurotox res* 5:579–598.

Prince, M., Bryce, R., Albanese, E., Wimo, A., Ribeiro, W., & Ferri, C. P. (2013). The global prevalence of dementia: A systematic review and meta-analysis. *Alzheimer's & Dementia*, 9(1), 63-75.

- Raghu P, Sivakumar B (2004) Interactions amongst plasma retinol-binding protein, transthyretin and their ligands: implications in vitamin A homeostasis and transthyretin amyloidosis. *Biochimica et Biophysica Acta (BBA) - Proteins and Proteomics* 1703:1–9.
- Richard IH et al. (2012) A randomized, double-blind, placebo-controlled trial of antidepressants in Parkinson disease. *Neurology* 78:1229–1236.
- Ross-Innes CS, Stark R, Holmes KA, Schmidt D, Spyrou C, Russell R, Massie CE, Vowler SL, Eldridge M, Carroll JS (2010) Cooperative interaction between retinoic acid receptor- and estrogen receptor in breast cancer. *Genes & Development* 24:171–182.
- Rouillard AD, Gundersen GW, Fernandez NF, Wang Z, Monteiro CD, McDermott MG, Ma'ayan A (2016) The harmonizome: a collection of processed datasets gathered to serve and mine knowledge about genes and proteins. *Database* 2016:100.
- Sanna G, Del Giudice MG, Crosio C, Iaccarino C (2012) LRRK2 and vesicle trafficking. *Biochemical Society Transactions* 40:1117–1122.
- Schrag A, Schott JM (2006) Epidemiological, clinical, and genetic characteristics of early-onset parkinsonism. *The Lancet Neurology* 5:355–363.
- Schulz-Schaeffer WJ (2010) The synaptic pathology of  $\alpha$ -synuclein aggregation in dementia with Lewy bodies, Parkinson's disease and Parkinson's disease dementia. *Acta Neuropathol* 120:131–143.
- Sharpe C, Goldstone K (2000a) The control of *Xenopus* embryonic primary neurogenesis is mediated by retinoid signaling in the neurectoderm. *Mechanisms of Development* 91:69–80.
- Sharpe C, Goldstone K (2000b) Retinoid signaling acts during the gastrula stages to promote primary neurogenesis. *Int J Dev Biol* 44:463–470.
- Shenefelt RE (1972) Morphogenesis of malformations in hamsters caused by retinoic acid: Relation to dose and stage at treatment. *Teratology* 5:103–118.
- Shum ASW, Poon LLM, Tang WWT, Koide T, Chan BWH, Leung Y-CG, Shiroishi T, Copp AJ (1999) Retinoic acid induces down-regulation of Wnt-3a, apoptosis and diversion of tail bud cells to a neural fate in the mouse embryo. *Mechanisms of Development* 84:17–30.
- Sidransky E, Lopez G (2012) The link between the GBA gene and parkinsonism. *The Lancet Neurology* 11:986–998.
- Smeyne RJ, Jackson-Lewis V (2005) The MPTP model of Parkinson's disease. *Molecular Brain Research* 134:57–66.

- Sockanathan S, Jessell TM (1998) Motor Neuron–Derived Retinoid Signaling Specifies the Subtype Identity of Spinal Motor Neurons. *Cell* 94:503–514.
- Sofroniew MV (2009) Molecular dissection of reactive astrogliosis and glial scar formation. *Trends in Neurosciences* 32:638–647.
- Spencer TE, Jenster G, Burcin MM, Allis CD, Zhou J, Mizzen CA, McKenna NJ, Onate SA, Tsai SY, Tsai M-J, O'Malley BW (1997) Steroid receptor coactivator-1 is a histone acetyltransferase. *Nature* 389:194–198.
- Stoney PN, Fragoso YD, Saeed RB, Ashton A, Goodman T, Simons C, Gomaa MS, Sementilli A, Sementilli L, Ross AW, Morgan PJ, McCaffery PJ (2016) Expression of the retinoic acid catabolic enzyme CYP26B1 in the human brain to maintain signaling homeostasis. *Brain Struct Funct* 221:3315–3326.
- Swindell EC, Thaller C, Sockanathan S, Petkovich M, Jessell TM, Eichele G (1999) Complementary Domains of Retinoic Acid Production and Degradation in the Early Chick Embryo. *Developmental Biology* 216:282–296.
- Takahashi, K. (1990). "Calpain substrate specificity," in *Intracellular Calcium- dependent Proteolysis*, eds R. L. Mellgren and T. Murachi (Boca Raton, FL: CRC Press), 55–74.
- Tang G, Qin J, Dolnikowski GG, Russell RM (2003) Short-term (intestinal) and long-term (postintestinal) conversion of  $\beta$ -carotene to retinol in adults as assessed by a stable-isotope reference method. *The American Journal of Clinical Nutrition* 78:259–266.
- Tang Y, Le W (2016) Differential Roles of M1 and M2 Microglia in Neurodegenerative Diseases. *Mol Neurobiol* 53:1181–1194.
- Thomas T, Thomas TJ (2001) Polyamines in cell growth and cell death: molecular mechanisms and therapeutic applications: CMLS, *Cell Mol Life Sci* 58:244–258.
- Thompson Haskell G, Maynard TM, Shatzmiller RA, Lamantia A-S (2002) Retinoic acid signaling at sites of plasticity in the mature central nervous system. *J Comp Neurol* 452:228–241.
- Tomac A, Lindqvist E, Lin L-FH, Ögren SO, Young D, Hoffer BJ, Olson L (1995) Protection and repair of the nigrostriatal dopaminergic system by GDNF in vivo. *Nature* 373:335–339.
- Valdenaire O, Maus-Moatti M, Vincent J-D, Mallet J, Vernier P (2002) Retinoic Acid Regulates the Developmental Expression of Dopamine D2 Receptor in Rat Striatal Primary Cultures. *Journal of Neurochemistry* 71:929–936.
- Verkhatsky, A., Rodríguez, J. J. & Steardo, L. (2014) Astrogliopathology: A Central Element of Neuropsychiatric Diseases? *Neuroscientist* 20, 576–588.

- Wagner E (2002) Retinoic Acid Synthesis in the Postnatal Mouse Brain Marks Distinct Developmental Stages and Functional Systems. *Cerebral Cortex* 12:1244–1253.
- White JA, Ramshaw H, Taimi M, Stangle W, Zhang A, Everingham S, Creighton S, Tam S-P, Jones G, Petkovich M (2000) Identification of the human cytochrome P450, P450RAI-2, which is predominantly expressed in the adult cerebellum and is responsible for all-trans-retinoic acid metabolism. *Proceedings of the National Academy of Sciences* 97:6403–6408.
- Wilson L, Gale E, Chambers D, Maden M (2004) Retinoic acid and the control of dorsoventral patterning in the avian spinal cord. *Developmental Biology* 269:433–446.
- Wolf JA, Stys PK, Lusardi T, Meaney D, Smith DH (2001) Traumatic Axonal Injury Induces Calcium Influx Modulated by Tetrodotoxin-Sensitive Sodium Channels. *J Neurosci* 21:1923–1930.
- World Health O. (2002) Projections of Mortality and Burden of Disease to 2030: Deaths by Income Group. Geneva.
- Xicoy H, Wieringa B, Martens GJM (2017) The SH-SY5Y cell line in Parkinson's disease research: a systematic review. *Mol Neurodegeneration* 12:10.
- XIE, Hong-rong; HU, Lin-sen; LI, Guo-yi (2010) SH-SY5Y human neuroblastoma cell line: *in vitro* cell model of dopaminergic neurons in Parkinson's disease, *Chinese Medical Journal*:123:8:1086-1092.
- Zetterström RH, Lindqvist E, De Urquiza AM, Tomac A, Eriksson U, Perlmann T, Olson L (1999) Role of retinoids in the CNS: differential expression of retinoid binding proteins and receptors and evidence for presence of retinoic acid: Role of retinoids in the CNS. *European Journal of Neuroscience* 11:407–416.
- Zhang W, Vreeland AC, Noy N (2016) The RNA-binding protein HuR regulates protein nuclear import. *Journal of Cell Science*:jcs.192096.
- Zolfaghari R, Mattie FJ, Wei C-H, Chisholm DR, Whiting A, Ross AC (2020) Using the human CYP26A1 gene promoter as a suitable tool for the determination of RAR-mediated retinoid activity. In: *Methods in Enzymology*, pp 561–590.

## 6. Appendices

6.1 Supplemental Data-Link- <https://umt.box.com/s/fckcgdp4swz3qpy24nei01y0enw2h284>

- qPCR graphs: All Experiments
- Foti et al., (2016) CYP26A1, CYP26B1 Homology Models (.pdb file)
- Niewiadowska-Cimicka et al., (2017) GWAS Lists- Analysis of RAR $\beta$  Binding Sites in Neurodegenerative Diseases
- Signaling Pathways of Interest